CHAPTER - II

PREPARATION AND CHARACTERIZATION OF NANOCRYSTALLINE FERRITES

To be surprised, to wonder, is to begin to understand.

To see a world in a grain of sand,

And a Heaven in a wild flower,

Hold Infinity in the palm of your hand

And eternity in an hour.

- William Blake

CHAPTER - II

PREPARATION AND CHARACTERIZATION

PART A : PREPARATION OF NANOCRYSTALLINE FERRITES

INTRODUCTION

Metallurgists and material scientists have been conducting researches over several centuries to develop materials which are stronger and lighter than the existing materials and also capable of use at elevated temperatures. Several novel and non-equilibrium processing methods have been developed during the past few decades to improve the performance of the existing materials. These include rapid solidification from the liquid state [1, 2], mechanical alloying [3], plasma processing [4], vapour deposition [5] etc.

A central underlying theme in all these methods is to energize the material to bring it into a highly non-equilibrium (metastable) state through melting, evaporation, irradiation, application of pressure, storing of mechanical energy etc. [6]. The material is then brought to another lower energy metastable state by quenching or related processes when it can exist as a supersaturated solid solution, metastable crystalline or quasi crystalline phase or even in a glassy state, affording ample opportunities to modify the crystal structures and/ or microstructures. These processes have led to considerable improvement in the properties

of a number of alloy systems and consequently some industrial applications.

A novel way of transforming a material to a metastable state is to reduce its grain size to very small values of a few nanometers (1 nm = 10^{-9}m), when the proportion of atoms in the grain boundaries is equivalent to or higher than those inside the grains. This type of metastability can be classified as morphological metastability. Materials with such small grain size are now referred to as nanocrystalline materials and have been shown to have properties vastly superior to those exhibited by conventional grain sized polycrystalline materials. It is the combination of unique compositions and novel microstructures that leads to the extra-ordinary potential of the nanocrystalline materials.

Increased activity on the synthesis of nanocrystalline materials in recent years dates back to the pioneering investigations of Herbert Gleiter of the University of Saarlandes in Germany in 1981 [7]. He synthesized ultrafine nanometer sized metallic particles using an inert gas condensation technique. Since then a number of techniques have been developed in which the starting material can be either in the solid, liquid or gaseous state.

Particle size range can be controlled from nanometer to micron size during the synthesis by controlling nucleation and growth of the particles. In case of magnetic materials it is observed that materials

having equal grain size exhibit different magnetic properties depending upon the method of preparation.

2.A.1 Classification of Methods :

The various methods of preparation can be broadly classified under three categories :

1. Physical
2. Chemical
3. Biological

1. Physical Methods :

a) Gas Aggregation of Monomers :

This method involves establishment of monomer population, cooling of monomers and growth of cluster by successive addition of monomers. Drawbacks involve the temperature limitation imposed by heating source and chemical reaction between metal and the refractory metal crucibles.

b) Ion Beam Method :

This method is based on thin film deposition technique where first clusters are produced by using sources like oven or laser and later they are ionized by electron beam to form stable crytals.

c) Inert Gas Evaporation Technique/ Gas Condensation Technique/ Consolidation :

This method involves evaporation of the metal or a mixture of metals inside an ultra high vacuum (UHV) chamber filled with Helium gas (9) A variety of evaporation methods and their effect on size, size distribution and constitution of the powder particle is studied by Gleiter [10] and Siegel [11].

The processing technique allows for great versatility. The composite materials can be produced by mixing two or more evaporation sources. Oxide or ceramic materials can be produced by mixing or replacing the inert gas with reactive gas. The disadvantage is that during collection of powder some particle agglomerates may be formed.

d. Mechanical Alloying :

It is a commercial technology to produce large quantities of materials. Mechanical alloying consists of repeated welding, fracturing and rewelding of powder particles in a dry high energy ball charge.

The common drawback is the increased impurity concentration due to the grinding with the walls of the container [13]. A major advantage is that it is a 'quality' process permitting several kilograms of materials to be produced in times upto 100 hours.

e. Sputtering :

This method is used to fabricate multilayered nanocomposite materials. Sputtering controls the layer thickness to fractions of a nanometer and can be used to make metallic or insulating samples.

2. Chemical Methods :

a. Micro Emulsion Method :

This is one of the technologies which allows overcoming of the problem of control of particle size. It consists of performing chemical synthesis of the materials in conditions of a restricted environment [15].

b. Sol-Gel Method :

Sol is prepared by mixing nitrates of metals whose ferrite is to be obtained and Si $(OC_2H_5)_4$ and concentrated nitric acid. The gelation takes place in nearly 48 hours, after which it is sintered for different periods of time to obtain nanocrystalline ferrites. Ni-Zn crystals having dimensions varying from 13 to 35 nm have been synthesized by sol-gel method [16].

c. Sol-Gel Auto Combustion Method :

A sol-gel auto combustion method is used by several researchers to synthesize spinel and pervoskite powder [17-27]. This is a novel way and unique combination of chemical sol-gel process and the combustion process. The process has the advantage of inexpensive precursors, a simple preparation method and a resulting nano sized powder.

3. Biological Methods :

Newer approaches involving biological methods or those that attempt to mimic biological methods (i.e. biomimetric) are being thoroughly investigated for the production of metal-based nanocrystallites. Generally these biological methods rely on the process of biomineralization [35-37]. New techniques like obtaining ferrites from stainless steel making solid waste [28] and from sulphuric pickling waste water have also been reported [29].

Nanocrystalline magnetic oxides have attracted the attention even of chemists who have developed techniques like combustion synthesis for the preparation of nanosize magnetic oxides due to their versatility [30].

2.A.2 Advantages of Chemical Synthesis :

1. Chemical synthesis route plays a crucial role in designing the final product as they are better and less cumbersome for the production of fine grained mixed oxide powders.

2. The use of chemistry in the preparation of materials can avoid three major problems- diffusion, impurities and agglomeration. The reasons being that the fine, chemically prepared powders allow for shorter diffusion distances and improved homogeneity. The chemical precursors used can be easily refined to increase the purity and careful control of solvent removal from the precursors will lead to the

production of crushable agglomerates. In the present synthesis a chemical route for the preparation of nanocrystalline ferrites is followed.

2.A.3 Fast Firing Method (Pramanik Method) :

Stoichiometric amounts of the individual metal nitrates are mixed thoroughly in accordance with desired composition to form the basic solution. 10% aqueous PVA and aqueous solution of sucrose are mixed together with thorough stirring. The resulting solution is evaporated at 200^0C. Complete evaporation of the solution occurs together with liberation of brown fumes of NO_2 and the formation of a highly viscous liquid. Further heating of the liquid causes decomposition to a voluminous organic based black, fluffy mass which is ground to fine powders to form the precursor material. Heat treatment of the precursor materials results in the formation of desired nanocrystalline oxides.

2.A.3.1 Role of Sucrose and PVA :

The sucrose in the solution serves two purposes First it provides a wrapping through co-ordination for the cations in solution and circumvents their selective precipitation from the solution during the evaporation process. The sucrose being always in excess to the metal ions works as a chelating agent and ensures atomistical distribution of the cations throughout the polymeric network structure.

$$C_{12}H_{21}O_{11} + M\,(No_3)_x + CCH\,(OH) - (H_2)_n \longrightarrow C + M_2O_x + NO_2$$

Second it serves as an efficient fuel for the combustion reaction being oxidized by the nitrate ions. Stability of the polymeric approach comes from the chemical bonding of the cations onto the polymeric chain and from the development of extremely high viscosity polymeric solution. Even as the chemical bonding is destroyed during pyrolysis the high viscosity favours low cation mobility which helps to affect the crystallite/ agglomerate morphology.

The aqueous solution of sucrose in presence of dilute nitric acid gets hydrolyzed to fructose and glucose that gets further oxidized to gluconic acid (or, a polyhydroxy acid).

The gluconic acid has a carboxylic acid group in one end and fixed linear hydroxy groups which can participate in the complexation of metal ions and it may form branched polymer with PVA [33]. A schematic representation of the reaction is as shown.

Sucrose in presence of PVA in very small quantity (at 10%) gives rise to a crushable fluffy powder of the oxide system. The higher the fluffiness of the powder lower is the particle size.

The PVA provides a polymeric matrix structure for the cations and also provides heat through combustion of the carbonaceous material remaining of oxidized PVA. In addition it helps in the poly condensation reaction in presence of oxidized saccharides and gives rise to a branched chain polymer network structure where the metal on (M^{+x})

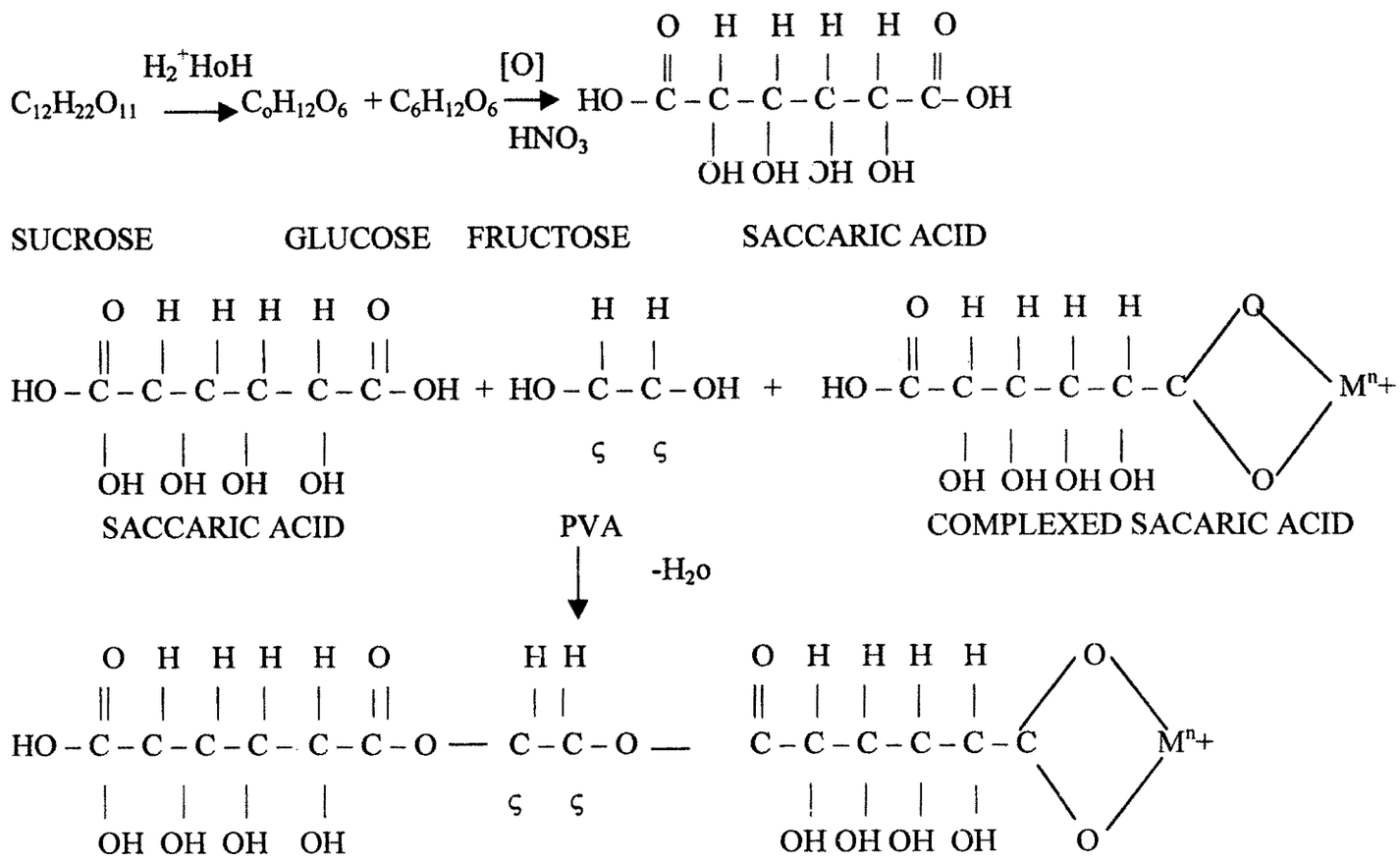

PART OF POLYMERIC RESIN

are held in the hydroxylic pockets of the branch chain through complex formation. The pyrolysis of these branched chain polymer would release various gases from the pocket making the structure highly porous and fluffy.

2.A.4 Actual Preparation of Samples :

1. To prepare 10% PVA solution :

To prepare the solution of PVA (polyvinyl alcohol) 20gm of solid PVA was dissolved in 200ml of distilled water. The mixture was stirred well using a magnetic stirrer for half an hour at 80^0C to get clear solution.

2. Beaker A :

Contains 10ml PVA + 50ml distilled water + 30gm sucrose. This composition is heated slowly using magnetic stirrer to get the clear solution.

3. Beaker B :

The given quantity of metal nitrates are dissolved in 50ml of distilled water to get a homogenous solution. Solution B is slowly added to solution A. The mixture is kept on magnetic stirrer and heated at about 80^0C to 1.5 hours.

NO_2 fumes are released during the process and a viscous mixture is formed. The viscous mixture is transferred to a beaker where

evaporation takes place. During evaporation many processes take place and lastly the powder burns like live charcoal undergoing oxidation to form the ferrite in powder form.

The ferrite samples with the general formula $Ni_{0.7-x}$ Mg_x $Zn_{0.3}Fe_2O_3$, with x = 0.1, 0.2. 0.3, 0.4, 0.5 were prepared using the combustion technique. The mixture was presintered at 800^0C for 8 hours in air medium.

The pellets were prepared by pressing the powder in a die of 1.5cm dia meter with the help of hydraulic press by applying the pressure of about 6 to 8 tonnes per square inch for about 5 to 10 min. The final sintering was carried out at 900^0C for about 12 hrs. in air medium to densify the pellets.

14411

PART – B : STRUCTURAL ANALYSIS BY X-RAY DIFFRACTION

INTRODUCTION

X-ray diffraction is a versatile non-destructive analytical technique for identification of the constituents in multiphase mixtures (solid or powders samples) qualitatively and also for quantitative estimation of various crystalline forms. It also provides the information about amorphous content of the sample crystallite sizes, crystallinity, solid solutions, stress and texture.

X-ray diffraction method was developed by Bertaut [41], Warren and Aberbach [42]. This method is also applicable for the determination of crystalline size distribution of materials.

The spinel structure of $MgAl_2O_4$ was first confirmed by Bragg [43] using X-ray diffraction. Electron and Neutron diffraction are also employed in determining the crystal structure of ferrites. The neutron diffraction study of ferrite is carried out by a number of workers [44-46].

In the present study X-ray diffraction is used to –

1. Confirm the formation of ferrite.
2. Observe the impurity phases.
3. Determine the lattice constant, interplanar distances. Site radii and bond length etc.

2.B.1 Principle of X-ray Diffraction :

In X-ray analysis, a monochromatic X-radiation is allowed to fall on certain crystal planes containing atoms. According to Bragg, diffraction is possible only when the wavelength of X-rays is comparable with the path difference. We have Bragg condition as

$$2d \, \mathrm{Sin}\theta = n\lambda \qquad \ldots \qquad (2.1)$$

where n - integral number termed as order of diffraction

d - interplanar distance

θ - angle of diffraction

λ - wavelength of monochromatic x-ray

For a cubic structure interplanar distance 'd', the lattice constant 'a' and the Miller indices 'h k l' of reflecting planes are related by

$$d = a / (h^2 + k^2 + l^2)^{1/2} \qquad \ldots \qquad (2.2)$$

substituting the value of d from equation (2.2) into equation (1) and rearranging we get –

$$a = n\lambda \, (h^2 + k^2 + l^2)^{1/2} \; / \; 2\mathrm{Sin}\theta \qquad \ldots \qquad (2.3)$$

using equation (2.3) lattice parameter 'a' can be calculated for the first order. The above equation after squaring reduces to

$$[h^2 + k^2 + l] = \left(\frac{4a^2}{\lambda^2} \right) \mathrm{Sin}^2\theta \qquad \ldots \qquad (2.4)$$

For a particular sample $4a^2/\lambda^2$ is constant. The different peaks correspond to different values of θ, from which the values of $S = (h^2 + k^2 + l^2)$ is determined.

For cubic samples, it is possible to calculate the radii of tetragonal (A) and octahedral (B) sites with the help of relations

$$\left.\begin{aligned} r_A &= (U - 1/4)\, a\sqrt{3} - Ro \\ \text{and} \quad r_B &= (5/8 - u)\, a - Ro \end{aligned}\right\} \qquad (2.5)$$

The bond lengths were calculated by using the equations

$$R_A = \sqrt{3}\,(\delta + 1/8)$$

$$\text{and} \quad R_B = a\,(1/16 - \delta/2 + 3\delta^2)^{1/2} \qquad (2.6)$$

Where δ - deviation from oxygen parameter (u)

δ - $u - u_{ideal}$

u - 0.381 A^0 for Ni ferrite and

$U_{ideal} = 0.375\ A^0$

Ro - radius of oxygen ion = 1.35 A^0

The particle size of the spinel phase has been estimated from the broadening of the X-ray diffraction peaks using the Scherrer equation

$$d = 0.9\,\lambda / \beta \cos\theta \qquad .. \qquad (2.7)$$

β - half peak width

2.B.2 X-ray Diffraction Methods

The Laue method rotating crystal method and powder method are the diffraction methods used in practice. The details of these methods have been discussed in the literature [47, 48]. Out of these the powder method is well suited for polycrystalline samples.

The powder method was developed by Debeye and Scheerrer [49] and Hull [59] independently. In this method the crystal to be examined is reduced to a very fine powder and placed in a beam of mono-chromatic x-rays. Each particle of powder is a tiny crystal oriented at random with respect to the incident beam. The result is that every set of lattice planes will be capable of reflection. This method is widely used in the study of ferrites. Krishnamurthy [51] has used this method to find the cation distribution of Ni-Zn ferrites. Srivastava et al. [50] have reported the exchange constants in spinel ferrites and lattice parameters of Ni ferrites. Satyamurty et al. [53] have studied Y-K angle in nickel zinc ferrite and obtained lattice parameters for these ferrites employing neutron diffraction technique. Bhise et al. [54] have reported IR and magnetization studies of Ni-Zn ferrites and have obtained lattice parameters using XRD technique. Srinivasan et al. [55] have reported magnetic properties of high density of Ni-Zn ferrites characterising the compositions by X-ray analysis.

2.B.3 Experimental Technique :

The X-ray diffraction patterns of all the samples were taken by using Cu kα radiation of wavelength 1.5418 A^0 on Philips PW 1710 diffractometer [at Common Facility Centre, Shivaji University, Kolhapur]. The sample in the form of powder was spread uniformly on a mounted screen of the sample holder, so as to form a plane surface of the specimen. The powder having tiny crystallites at different orientations diffract the monochromatic X-rays. The diffraction maxima occur only when the Bragg's condition is satisfied. The X-ray diffractograms of the present samples were recorded at a slow speed (1 degree per min) of goniometer and the scanning angle varied from 10^0 to 90^0. Indexing was done by comparing the observed data with ASTM data available for spinel ferrites. The spinel lattice gives rise to diffraction peaks with particular specific indices.

Table 2.B.1

X-ray Diffraction data of $Ni_{0.6}Mg_{0.1}Zn_{0.3}Fe_2O_3$

$\lambda = 1.5418\ A^0$ $a = 8.369\ A^0$

Sr. No.	2θ	θ	Sinθ	d_{obs}	d_{cal}	hkl
1.	30.285	15.14	0.2612	2.9511	2.9511	(220)
2.	35.685	17.84	0.3064	2.5159	2.5159	(311)
3.	43.270	21.63	0.3686	2.0909	2.0909	(400)
4.	53.630	26.81	0.4511	2.7088	1.7088	(422)
5.	57.195	28.59	0.4786	1.6105	1.6105	(511)
6.	62.755	31.37	0.5206	1.4805	1.4805	(440)

Table 2.B.2

X-ray Diffraction data of $Ni_{0.5}Mg_{0.2}Zn_{0.3}Fe_2O_3$

$\lambda = 1.5418\ A^0$ $a = 8.359\ A^0$

Sr. No.	2θ	θ	Sinθ	d_{obs}	D_{cal}	hkl
1.	30.355	15.16	0.2616	2.9463	2.9550	(320)
2.	35.660	17.83	0.3016	2.5176	2.5200	(311)
3.	43.320	21.66	0.3690	2.0886	2.0895	(400)
4.	53.775	26.88	0.4522	1.7046	1.7060	(422)
5.	57.210	28.60	0.4787	1.6101	1.6085	(511)
6.	62.815	31.40	0.5211	1.4793	1.4775	(440)

Table 2.B.3

X-ray Diffraction data of $Ni_{0.4}Mg_{0.3}Zn_{0.3}Fe_2O_3$

$\lambda = 1.5418\ A^0$ $a = 8.3615\ A^0$

Sr. No.	2θ	θ	Sinθ	d_{obs}	d_{cal}	Hkl
1.	30.245	15.12	0.2608	2.9549	2.9598	(220)
2.	35.610	17.80	0.3059	2.5211	2.5241	(311)
3.	43.255	21.62	0.3685	2.0951	2.0920	(400)
4.	53.620	26.81	0.4510	1.7091	1.7088	(422)
5.	57.075	28.53	0.4777	1.6136	1.6111	(511)
6.	62.785	31.39	0.5208	1.4794	1.4798	(440)

Table 2.B.4

X-ray Diffraction data of $Ni_{0.3}Mg_{0.4}Zn_{0.3}Fe_2O_3$

$\lambda = 1.5418\ A^0$ $a = 8.364\ A^0$

Sr. No.	2θ	θ	Sinθ	d_{obs}	d_{cal}	Hkl
1.	30.260	15.13	0.2610	2.9536	2.9511	(220)
2.	35.625	17.81	0.3078	2.5045	2.5118	(311)
3.	43.200	21.6	0.3681	2.0942	2.044	(400)
4.	53.550	26.77	0.4504	1.7115	1.7073	(422)
5.	57.110	28.55	0.4779	1.6130	1.6096	(511)
6.	62.090	31.34	0.5201	1.4822	1.4785	(440)

Table 2.B.5

X-ray Diffraction data of $Ni_{0.2}Mg_{0.5}Zn_{0.3}Fe_2O_3$

$\lambda = 1.5418\ A^0$ $a = 8.367\ A^0$

Sr. No.	2θ	θ	Sinθ	d_{obs}	d_{cal}	Hkl
1.	30.350	15.175	0.2617	2.9449	2.9585	(220)
2.	35.700	17.80	0.3065	2.5144	2.5229	(311)
3.	43.325	21.66	0.3691	2.0883	2.0918	(400)
4.	53.670	26.83	0.4514	1.7077	1.7080	(422)
5.	57.155	28.57	0.4783	1.6115	1.6103	(511)
6.	62.745	31.37	0.5205	1.4807	1.4711	(440)

Table 2.B.6

Lattice Parameters

X	a, A^0
0.1	8.369
0.2	8.359
0.3	8.361
0.4	8.364
0.5	8.367

Table 2.B.7

Particle Size $Ni_{0.7-X}Mg_xZn_{0.3}Fe_2O_4$

X	Particle Size A^0
0.1	283
0.2	280
0.3	280
0.4	301
0.5	292

2.B.4 Results and Discussion :

The X-ray diffraction patterns of $Ni_{0.7-x}Mg_xZn_{0.3}Fe_2O_4$ for (x= 0.1 – 0.5) are as shown in the figs. 2.B.1 – 2.B.5.. It can be observed that–

1. There are no extra lines which confirms single phase ferrite formation.

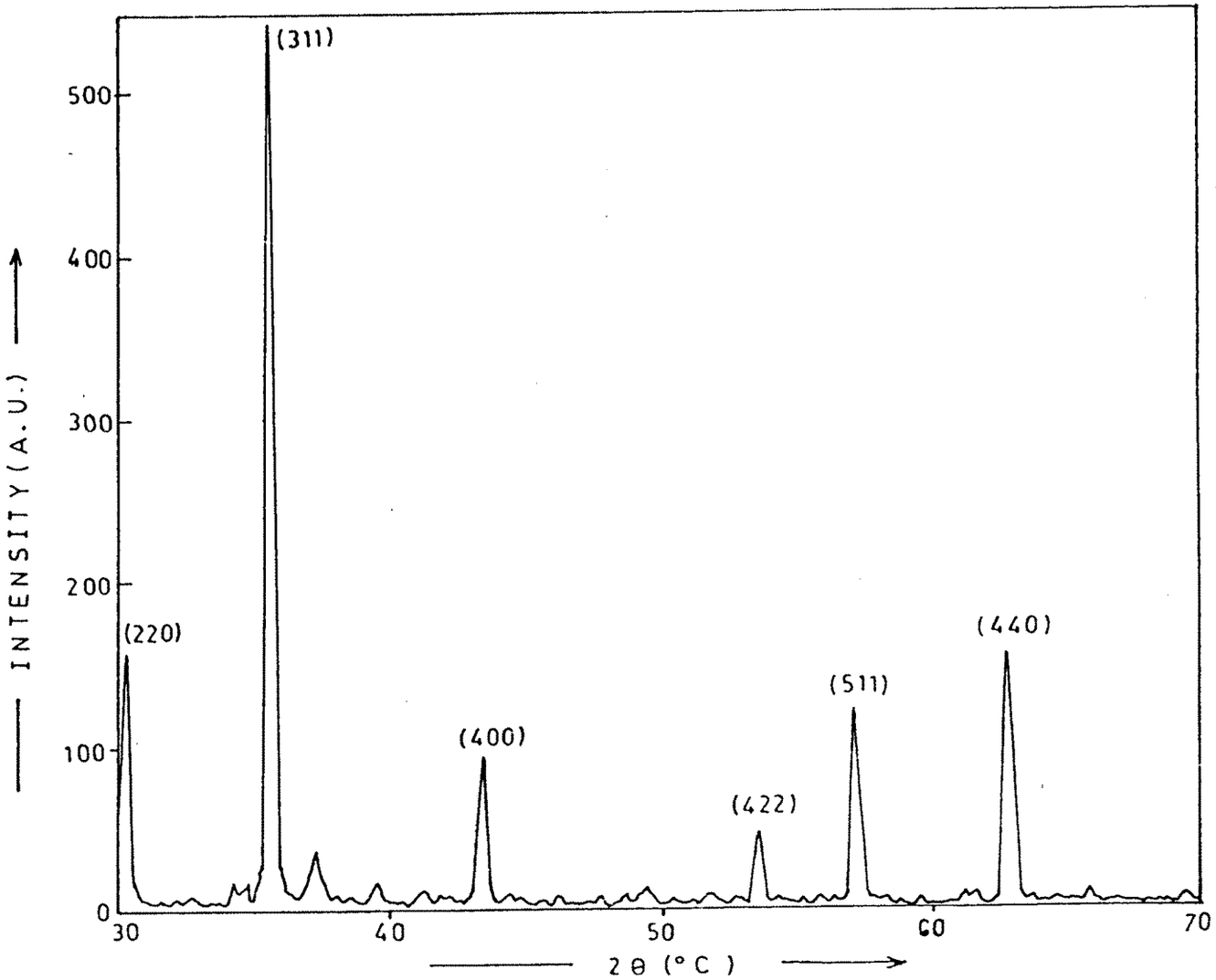

FIG. 2B: X-RAY DIFFRACTION PATTERN OF $Ni_{0.6}Mg_{0.1}Zn_{0.3}Fe_2O_4$ -

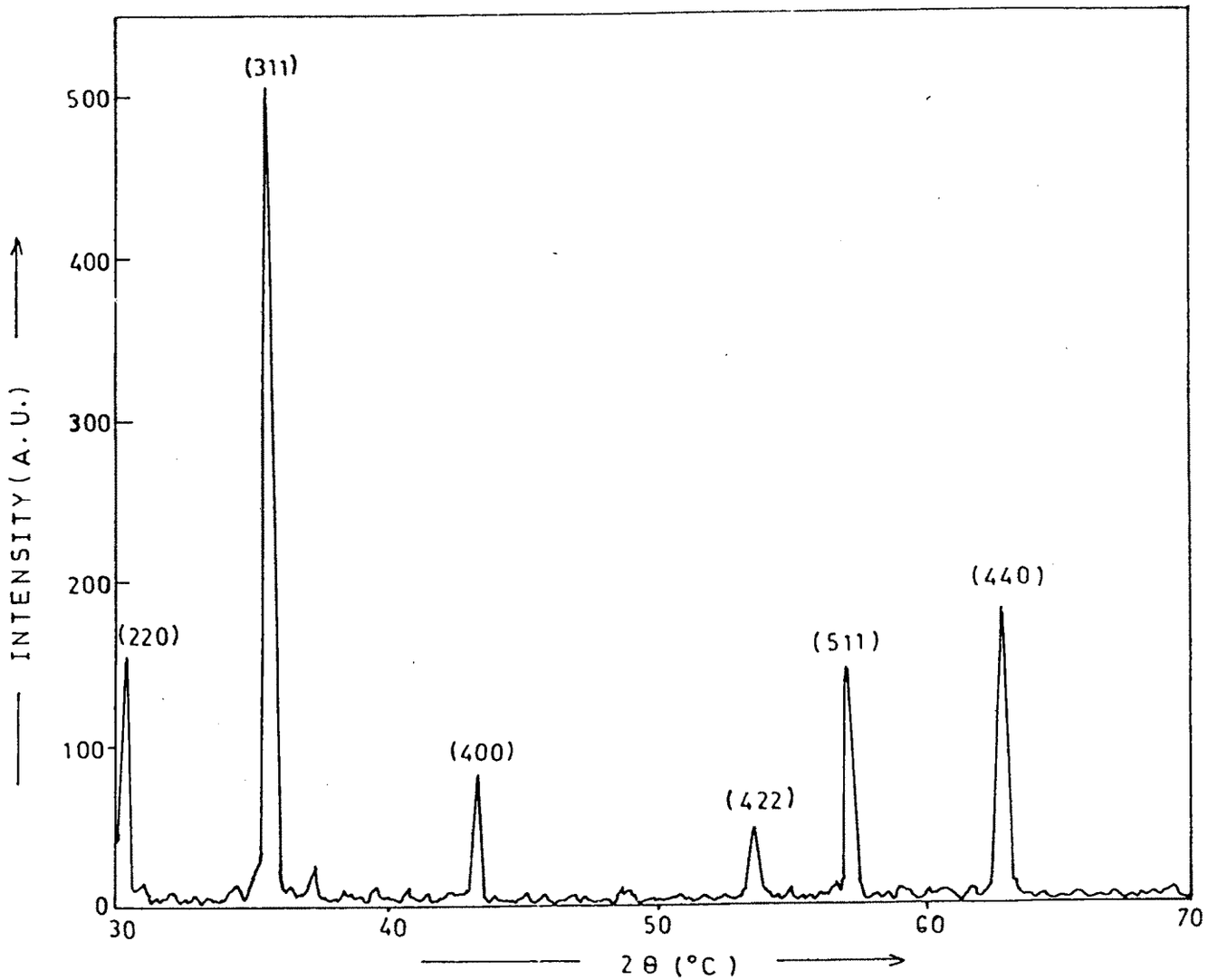

FIG. 2.B2 X-RAY DIFFRACTION PATTERN OF $Ni_{0.5}Mg_{0.2}Zn_{0.3}Fe_2O_4$.

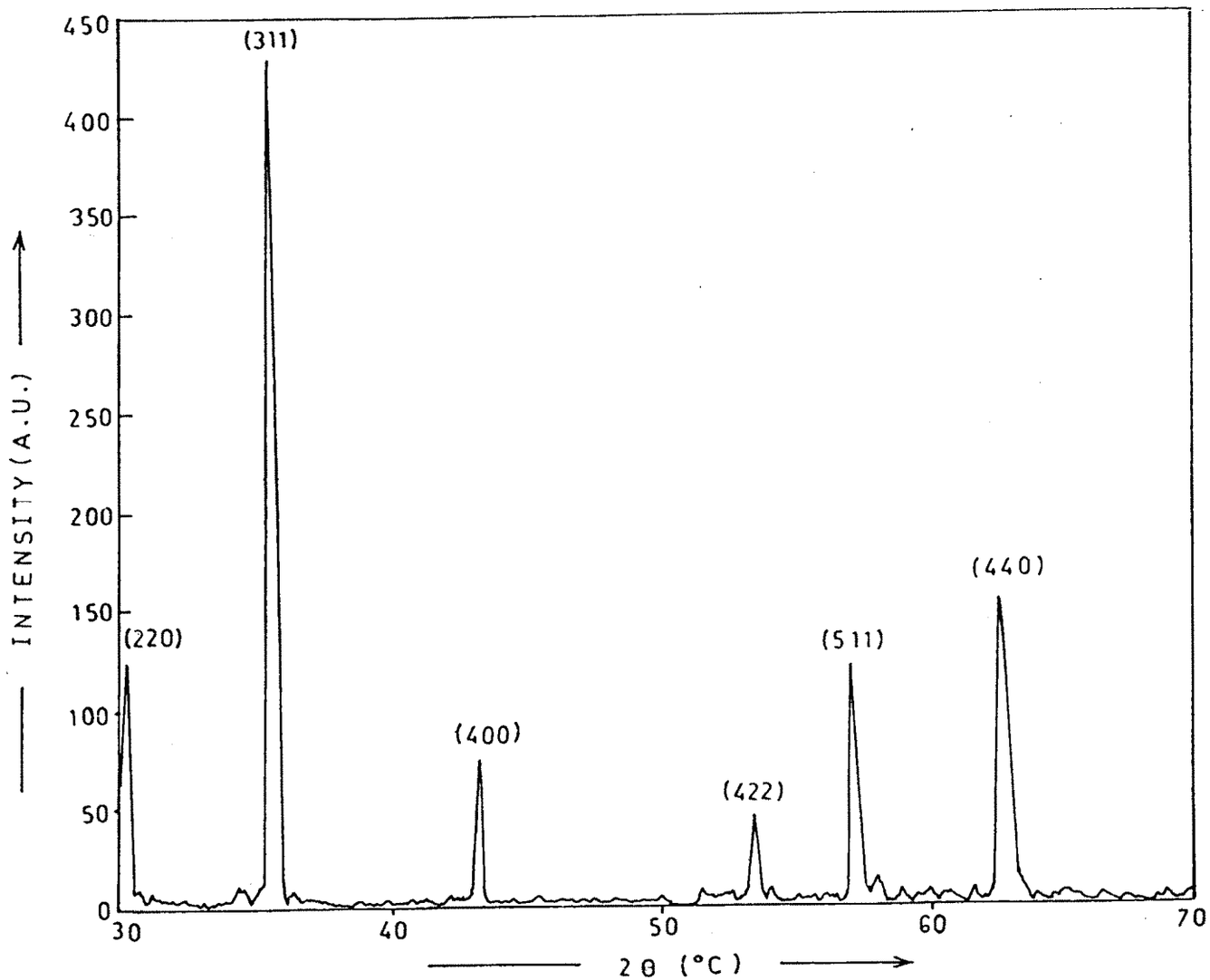

FIG. 3.33 X-RAY DIFFRACTION PATTERN OF $Ni_{0.4}Mg_{0.3}Zn_{0.3}Fe_2O_4$.

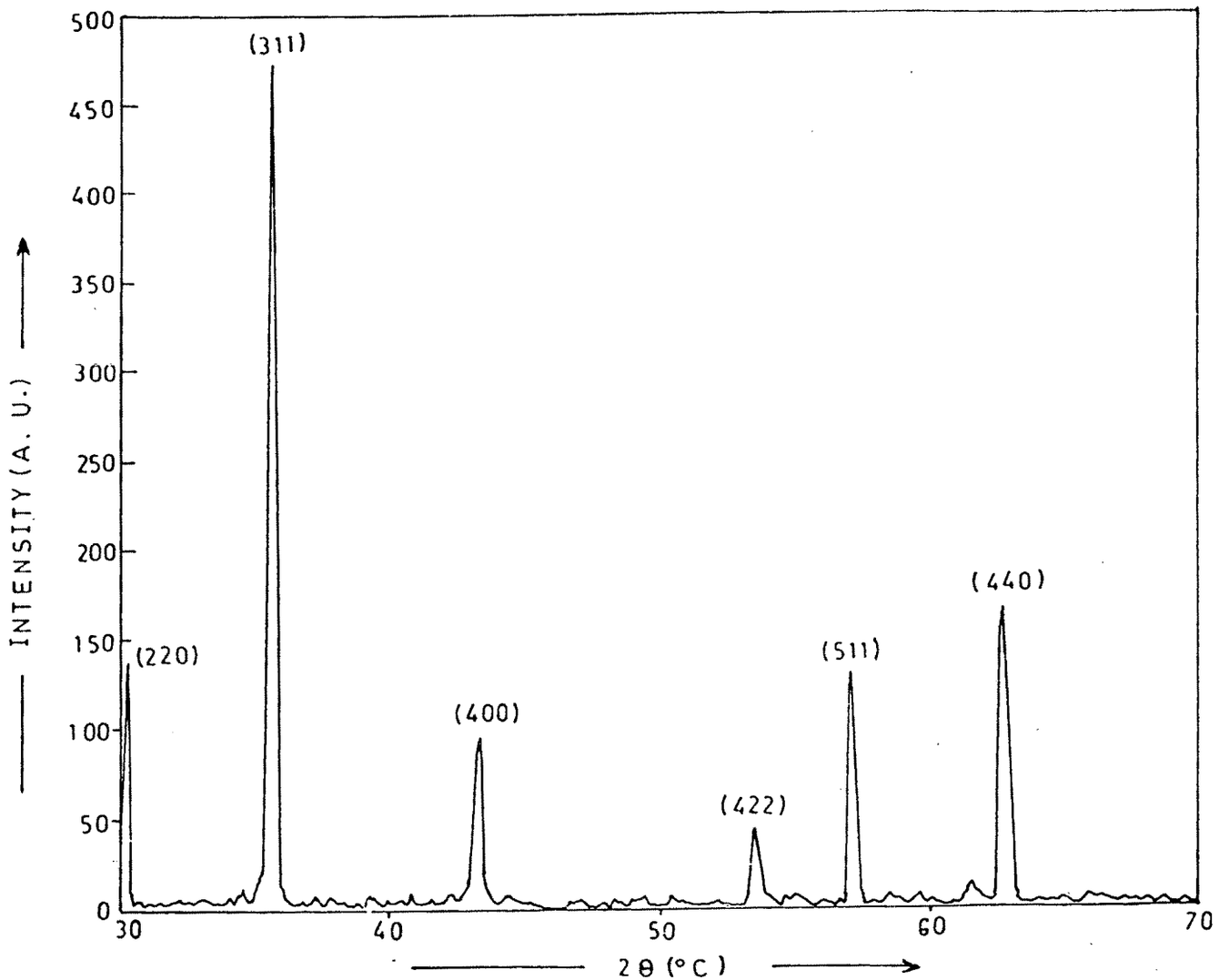

FIG. 2.B4 X RAY DIFFRACTION PATTERN OF $Ni_{0.3}Mg_{0.4}Zn_{0.3}Fe_2O_4$.

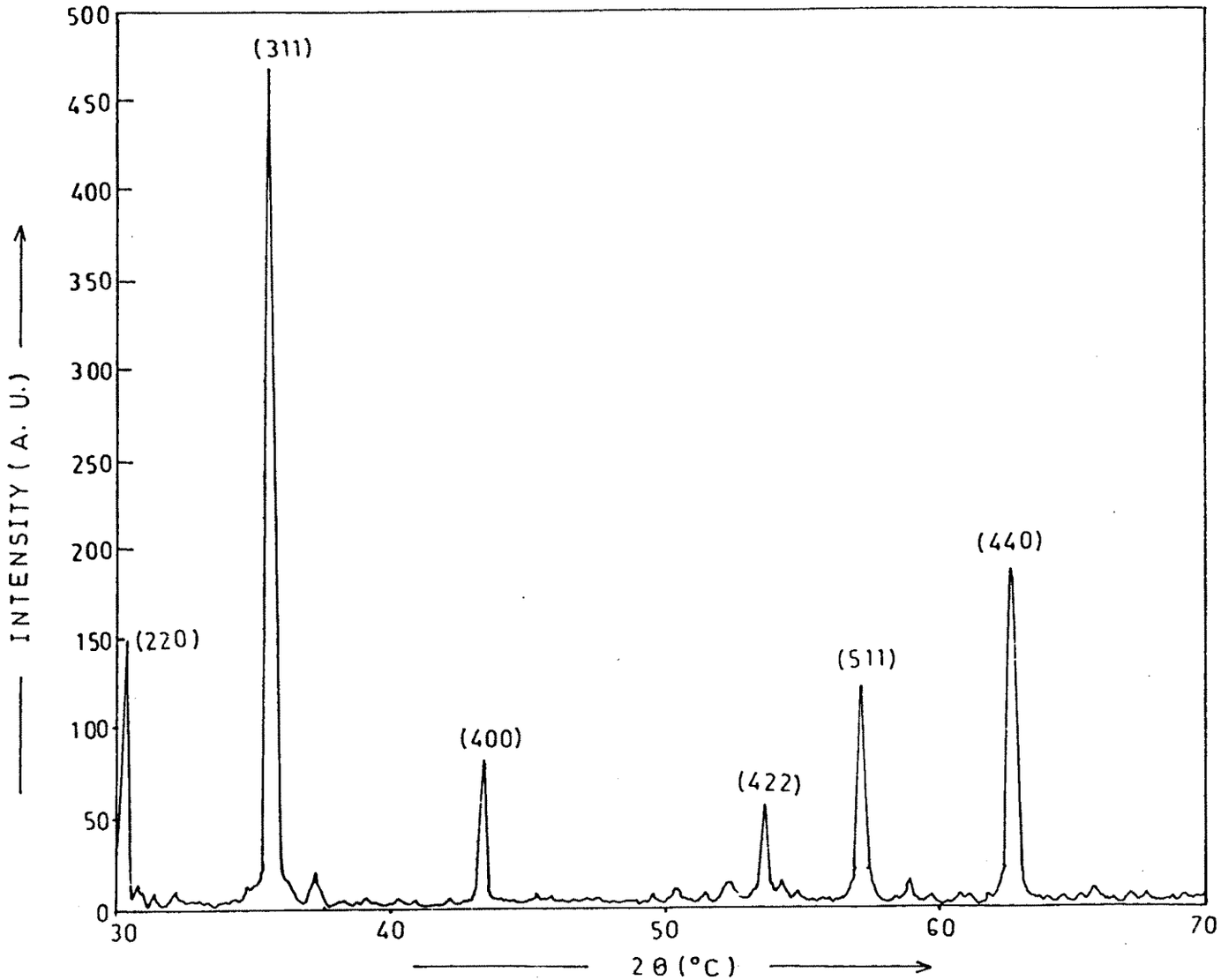

FIG. 2.B.5 X-RAY DIFFRACTION PATTERN OF $Ni_{0.2}Mg_{0.5}Zn_{0.3}Fe_2O_4$.

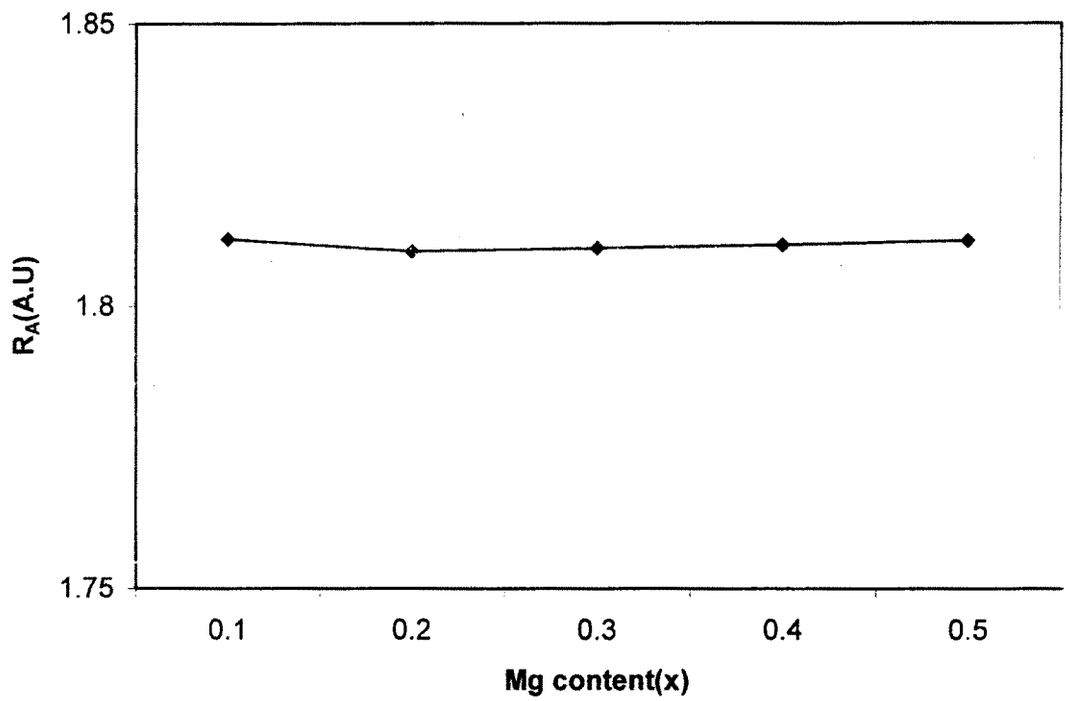

Fig 2.B.11 Variation of bond length (R_A) with Mg content

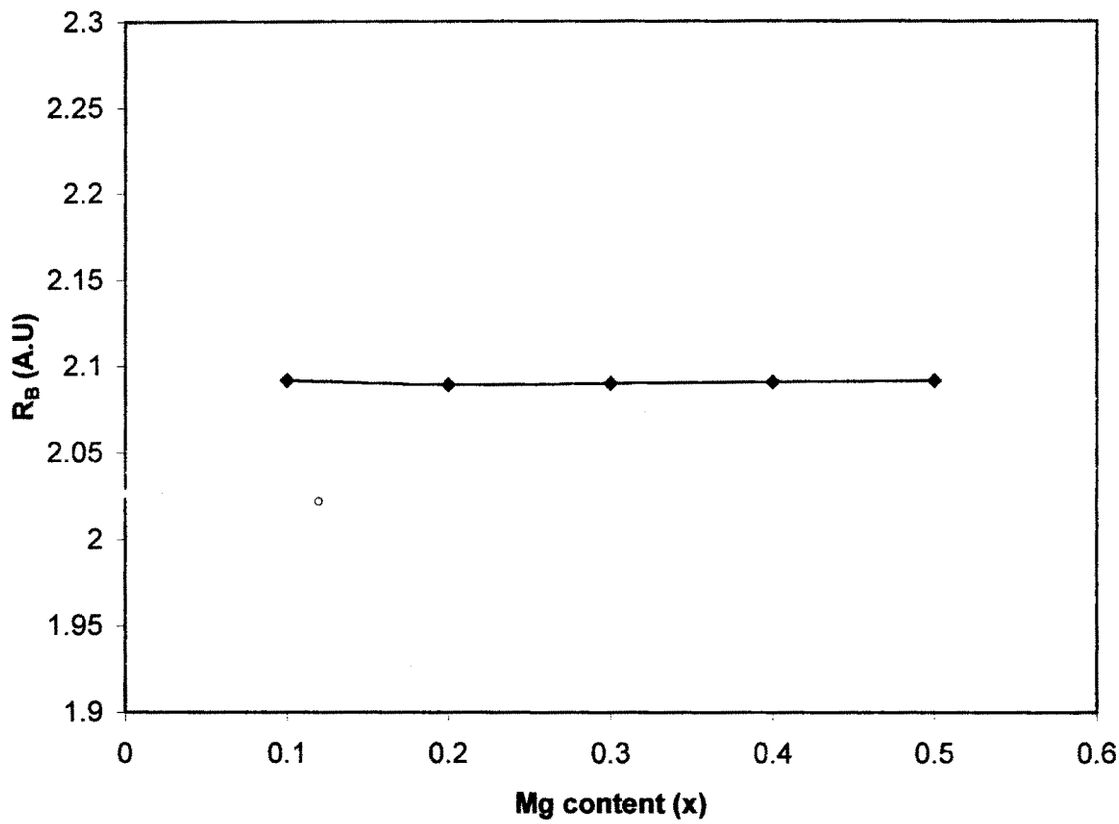

Fig.2.B.12 Variation of bond length (R_B) with Mg content

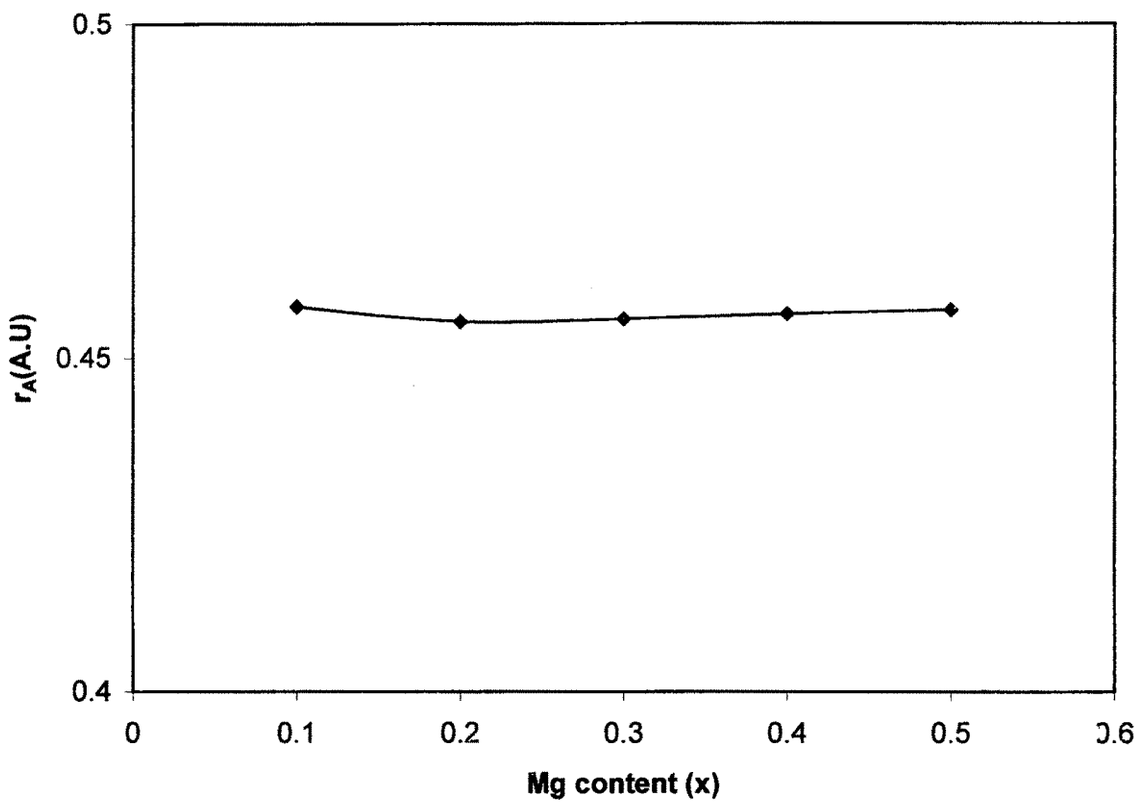

Fig.2.B.13 Variation of site radius (r_A) with Mg content

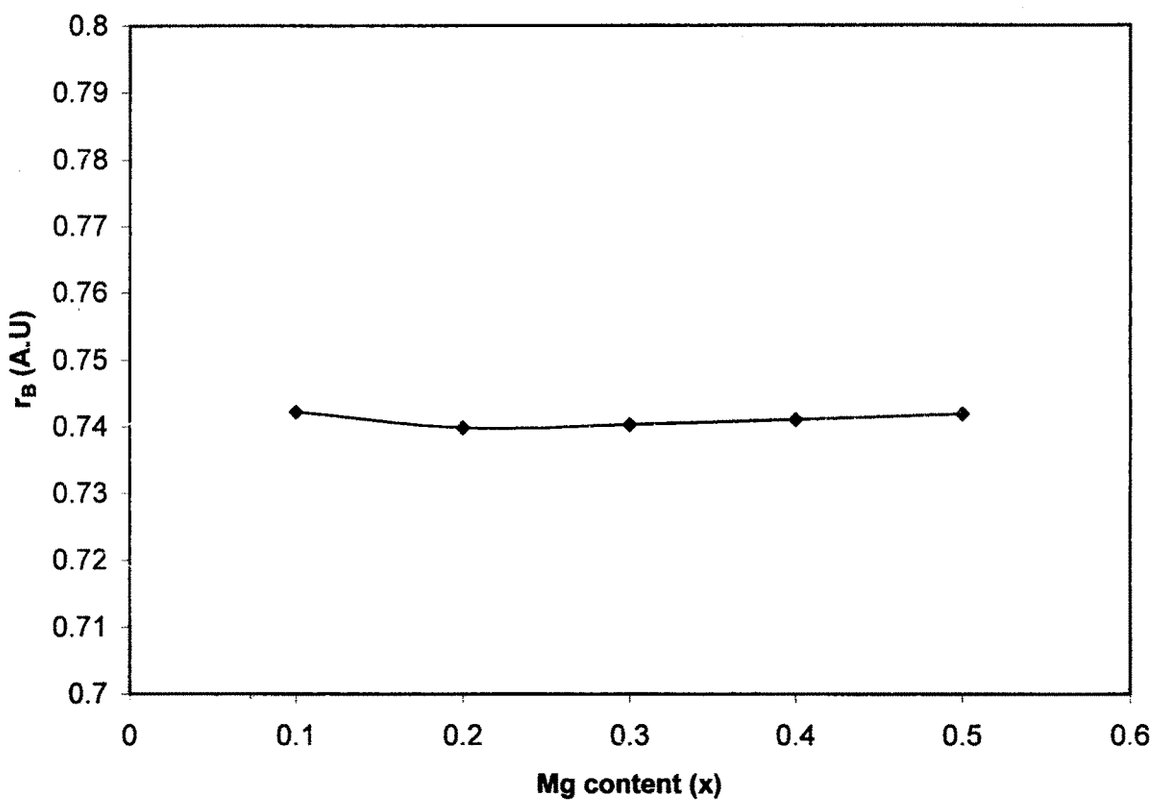

Fig.2.B.14 Variation of site radius (r_B) with Mg content

2. The interplanar distance 'd' for each diffraction angle was calculated using the relation (4). The observed and calculated 'd' values are given in the tables 2.B.1 – 2.B.5. It is seen that the observed and calculated 'd' values are in good agreement for all the indexed planes.

3. In case of all ferrites (311) reflections appears to be more intense. The other planes observed are (220), (400), (422), (511) and (440).

4. The lattice parameters for the samples are given in tables 2.B.1 – 2.B.5, which do not show any marked change. This is attributed to the fact that in the system Ni^{2+} with ionic radius of $0.74A^0$ is substituted by Mg^{2+} with ionic radius $0.75A^0$. As there is no change in the ionic radius of the substituted atom the lattice parameter does not change (Table 2.B.6).

5. The variation of bond length (R_A and R_B) and site radii (r_A and r_B) with Mg content is shown in the figures 2.B.11 – 2.B.14. It is observed that the site radii and bond length do not vary with composition (x) – [Table 2.B.8].

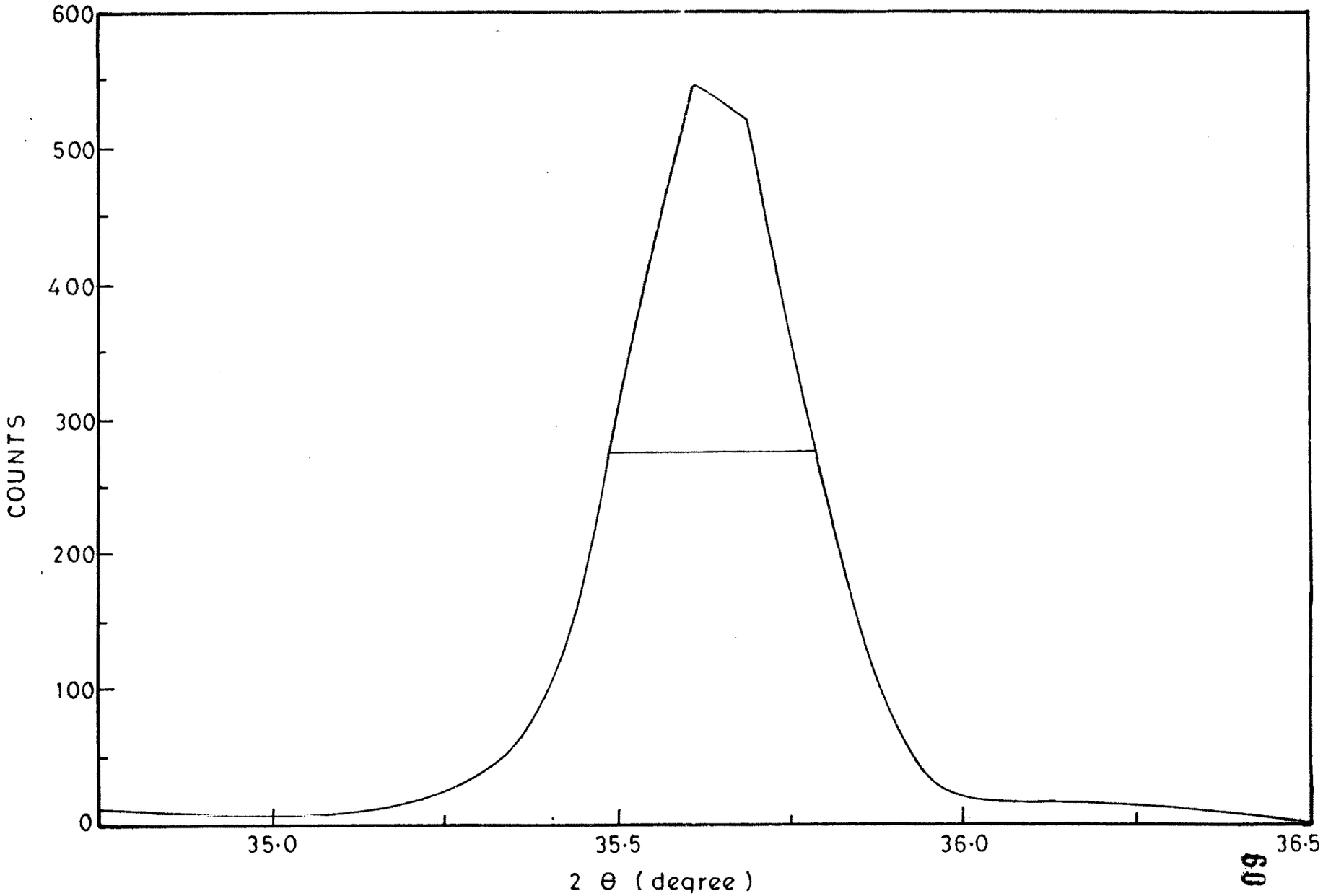

FIG.2·B·6-SLOW SCAN FOR X = 0·1

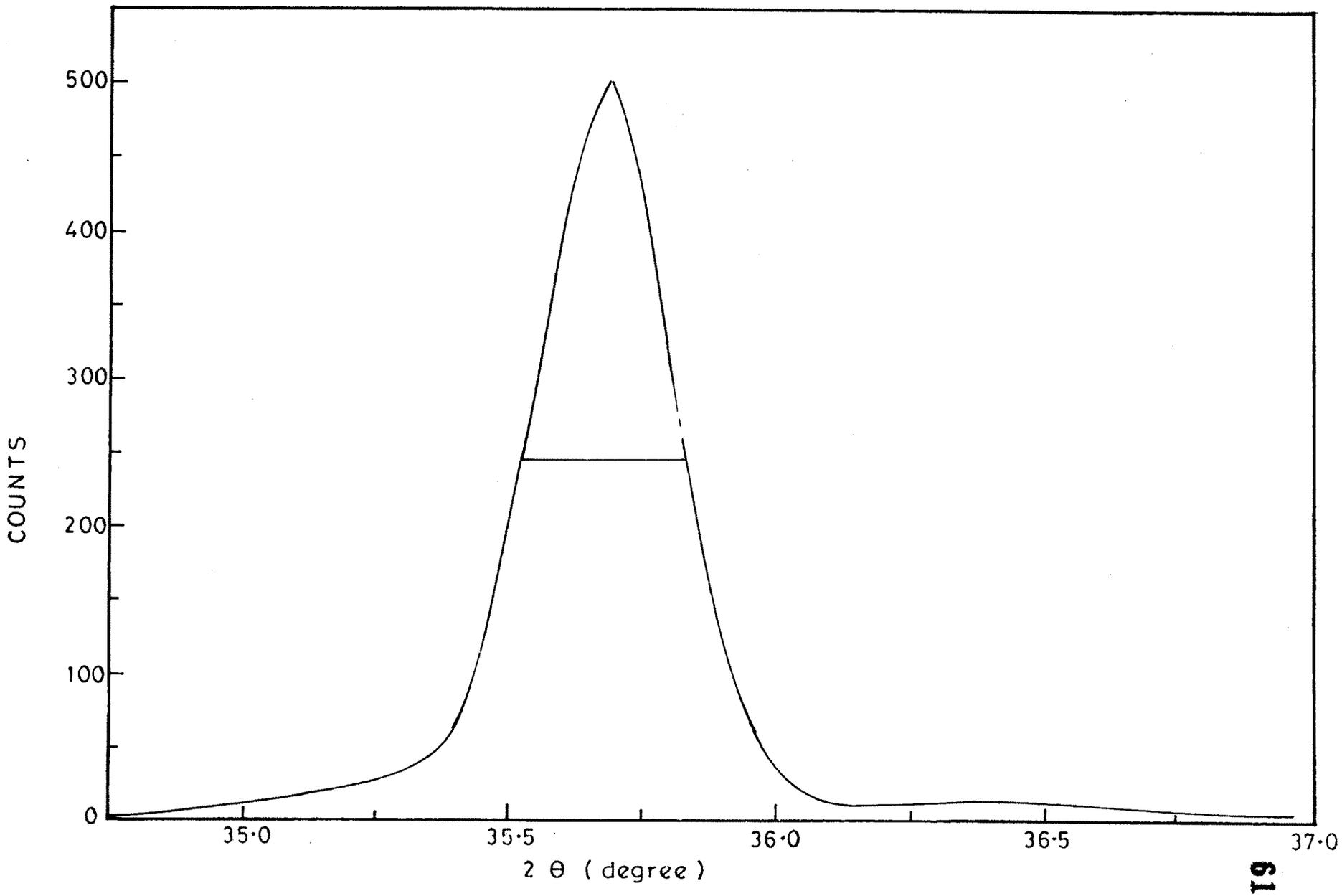

FIG.2·B·7-SLOW SCAN FOR X = 0·2

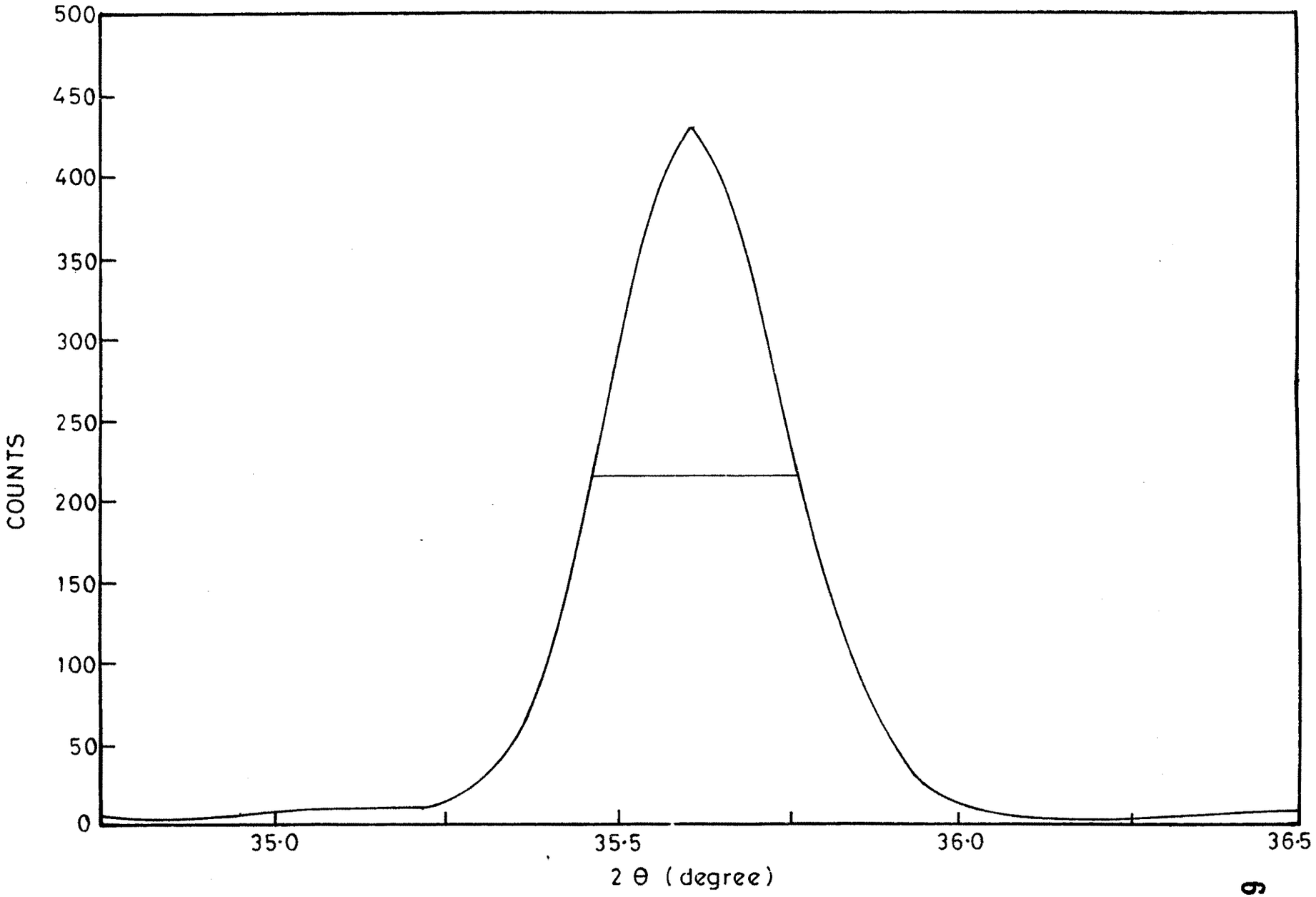

FIG. 2·B·8 – SLOW SCAN FOR X = 0·3

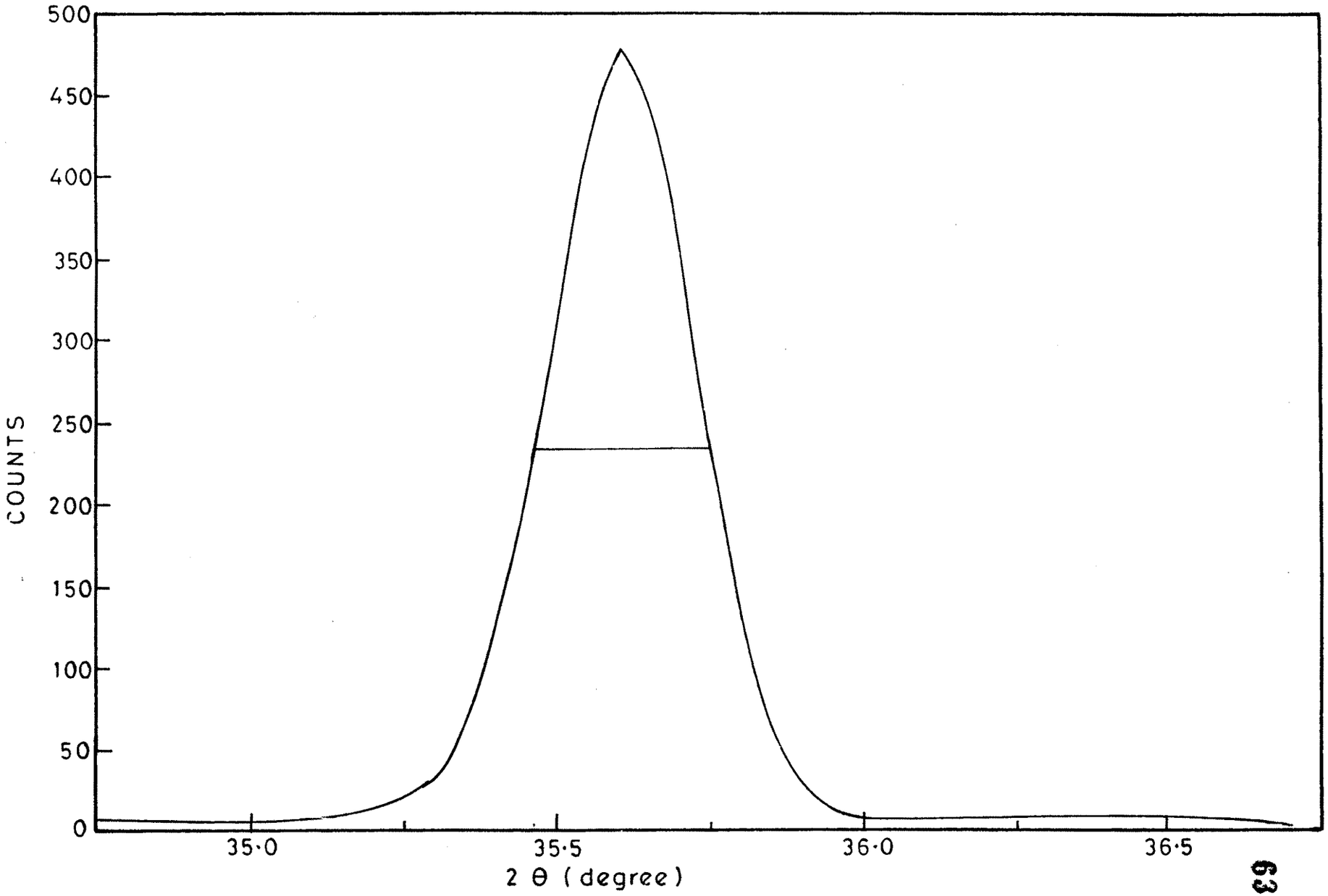

FIG.2·B·9 - SLOW SCAN FOR X = 0·4

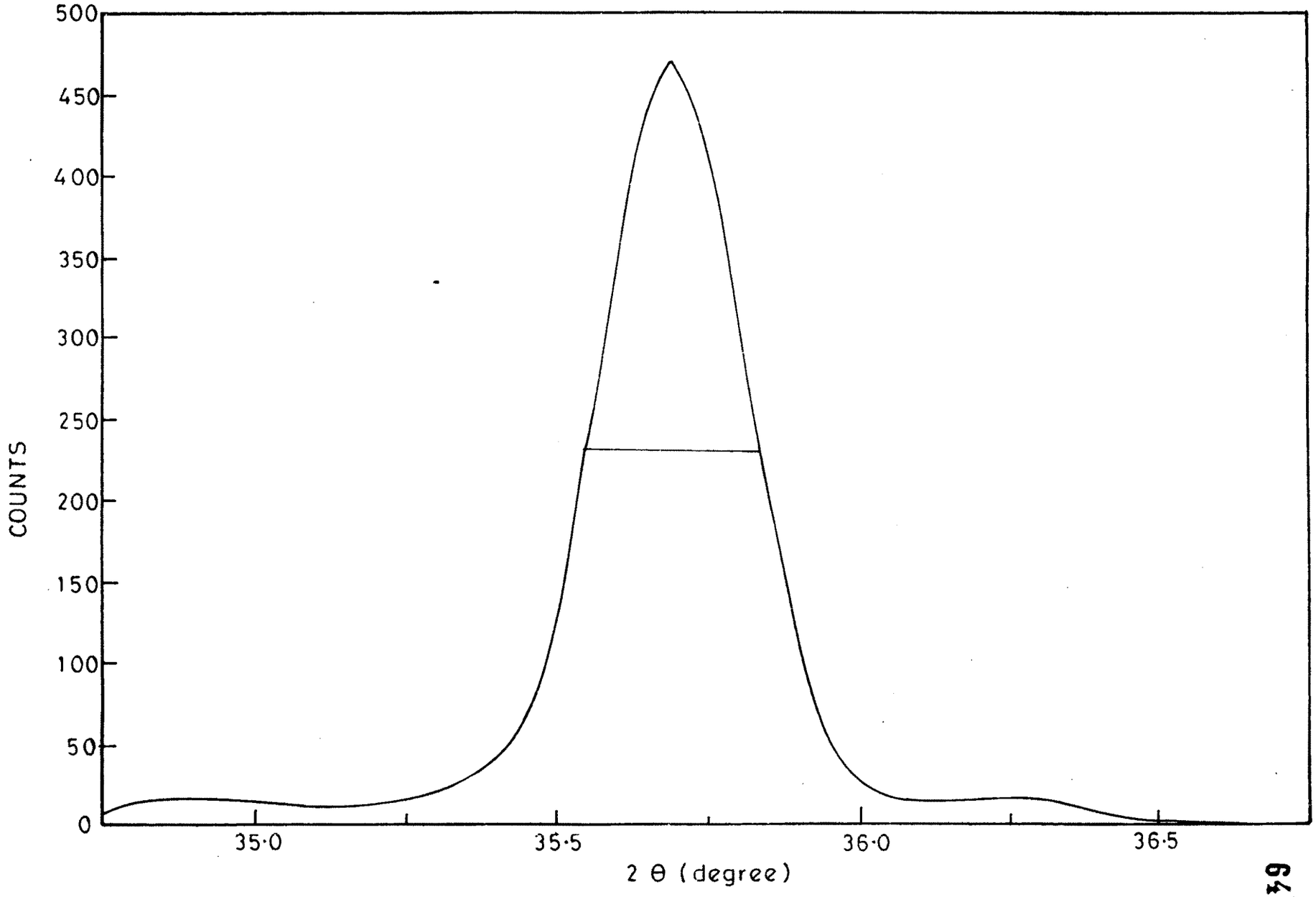

FIG.2·B·10-SLOW SCAN FOR X = 0·5

Table 2.B.8

Data on lattice parameter, bond length (R_A, R_B) and site radii (r_A, r_B) for $Ni_{0.7-x}Mg_x Zn_{0.3} Fe_2O_4$.

X	Lattice parameter (A^0)	R_A, A^0	R_B, A^0	r_A, A^0	r_B, A^0
0.1	8.369	1.8118	2.0923	0.4577	0.7422
0.2	8.359	1.8097	2.0898	0.4555	0.7398
0.3	8.361	1.8102	2.0903	0.4559	0.7403
0.4	8.364	1.8108	2.0910	0.4566	0.7410
0.5	8.367	1.8115	2.0918	0.4572	0.7418

This is again due to the fact that lattice parameter is approximately same and does not show any change on substitution of Mg^{2+}.

The bond length R_B is always greater than R_A. Similar results are reported in Al^{3+} substituted Ni-Zn ferrite [61]. The lattice parameters obtained in the present case are in close agreement with the lattice parameters of $Zn_{0.6}Ni_{0.4-x}Cu_x Fe_2O_4$ as reported by Deshmukh [56].

The particle size calculated by Scherrer equation (Figures 2.B.6 –10) and given in Table 2.B.7). They are in close agreement with Ni – Zn ferrites produced by other methods [57 – 60].

PART – C : SEM

INTRODUCTION

Most of the magnetic properties and characteristics of polycrystalline ferrites such as permeability, magnetic loss, hystersis loop, coercive force, rectangularity, energy product, resonance line width are microstructure sensitive [62] whereas crystalline anisotropy, magnetostriction, Curie temperature, saturation magnetization, ferromagnetic resonance, resistivity, elastic modulus, thermal expansion are microstructure independent [63]. At present, the microstructure sensitive properties of ceramic materials/ ferrites are controlled empirically by varying processing parameter so as to change grain size, porosity, size distribution etc.

An optimum microstructure depends on whether or not the domain walls are required to have high mobility [63]. A mobile domain pattern means avoiding any disturbance that can impede the movement of walls. A rigid domain pattern necessiates the presence of microstructural elements that effectively hinder movements. From physical research we know which microstructure is needed to obtain particular physical properties [64]. In general, it can be stated that a small grain size is needed when polycrystalline structure is essential. Examples are hard ferrites [65] and low loss high frequency ferrites [66].

The term microstructure has outgrown its original meaning, namely that structure which is seen through a microscope [67]. For

polycrystalline ferrites the term microstructure means the porosity, grain structures and phases detectable by micrographic analysis. The magnetic properties of soft ferrites are well understood [68, 69] in terms of porosity, grain size and other features of given microstructure.

2.C.1 Literature Survey :

In order to adequately characterize microstructure spatial dimensions and shapes of grains of which the polycrystalline material is built should be determined. This determination should be of statistical character because the grains forming the real polycrystalline material are differentiated in size and shape [70].

Roess [71] has pointed out that it is impossible to have both high permeability material and very low losses especially at higher frequencies. Limitations on desirable properties at high frequencies may more easily be overcome by control of microstructure than choice of chemistry. T. Postupolski [72, 73] has given topographical and geometrical approach to determination of spatial, granulametric, morphometric features of isotropic granular structure. H. P. Peloschek et al. [74] have carried out SEM studies on high permeability of Mn – Zn ferrites they have reported that a sintered body consisting of small grains prepared by normal method starting from fine powdered raw material of iron oxide or carbonate and zinc oxide exhibited statistical composition from grain to grain.

Ghate et al. have reviewed the boundary phenomenon in Mn – Zn soft ferrite in a book by Sudhal et al. [75]. Ghate has stated that grain boundaries influence properties by

1. Creating a high resistivity intergranular layer.
2. Acting as a sink for impurities that may serve as sintering aid and as grain growth modifiers.
3. Providing a path for oxygen diffusion which may modify the oxidation state of cations near the boundaries.

The permeability of high permeability ferrites is affected by the interaction of pores and boundaries, the types of boundary phase and microstresses.

P. Ravindranathan et al. [76] have carried out SEM studies and reported typical microphotograph of $Ni_{0.5}Zn_{0.5}Fe_2O_4$ ferrite composition prepared at 1000^0C.

J. G. Koh et al. [77] have reported typical microstructure photograph of

1. Basic composition - $Cu_{0.162}\ Fe_{0.054}\ Zn_{0.405}\ Mg_{0.405}\ Fe_{1.892}O_4$

in which 0.134 mol% $CaCO_3$ was doped and sintered at 1045^0C (B_3).

2. Basic Composition $Cu_{0.162}\ Fe_{0.054}\ Zn_{0.325}\ Mg_{0.325}\ Ni_{0.162}\ Fe_{1.892}\ O_4$ in which 0.134 mol% $CaCO_3$ was doped and sintered at 1035^0C (C_1).

They have reported that grain size of sintered specimen were larger than those of non sintered specimen with exception of specimen B and attributed increase of grain size for specimen B to compositional ingredient, thus showed different electrical properties from other specimen J. G. Koh et al. [78] have further reported typical microstructure photograph for following compositions.

A) $Zn_{0.485}Fe_{0.054}Mg_{0.407}Cu_{0.162}Fe_{1.946}O_4$ + 0.1 mol% NiO

A[1]) $Zn_{0.485}Fe_{0.054}Mg_{0.407}Cu_{0.162}Fe_{1.946}O_4$ + 0.1 mol% $CaCO_3$

B) $Zn_{0.503}Fe_{0.027}Mg_{0.262}Cu_{0.262}Fe_{1.973}O_4$ + 0.1 mol% NiO

B[1]) $Zn_{0.503}Fe_{0.027}Mg_{0.262}Cu_{0.262}Fe_{1.973}O_4$ + 0.1 mol% $CaCO_3$

T. Murase et al. [79] carried out studies on relaxation phenomena in Mg – Zn ferrites. They carried out microstructure studies on Cu Mg-Zn, Mg-Zn ferrites. They have reported that CuO addition in Mg-Zn accelerates grain growth and that the large grains of Mg-Cu-Zn ferrites contain pores and etch pits. They have further correlated grain growth and pores to decrease in μ_i with frequency.

D. N. Bhosale [80] carried out SEM studies on $Cu_{0.1}Mg_{0.4}Zn_{0.5}Fe_2O_4$ which were initially sintered and then on hot pressed samples. They have recorded that even after hot pressing grains did not appear to be fully grown because most of the grains were round and did not have sharp edges. However grains were large in size without significant intergranular porosity.

Cold pressed SEM photograph of some composition which did not exhibit any granular structure on hot pressing tends to favour the granular structure. It appeared that on increasing the temperature of hot pressing the grain structure improved. Because of hot pressing there was an improvement in initial permeability of the sample.

T. Nakamura [81] has reported SEM photograph of Ni- Zn – Cu ferrite, he showed that the ferrite grain size has a great influence on the domain well contribution, and it is necessary to increase the post sintering density and the ferrite grain size to increase domain wall susceptibility. Hongguo Zhang et al. [82] have investigated temperature dependence SEM photographs of $Ni_{0.15}Cu_{0.25}Zn_{0.6}$ $Fe_{1.96}O_4$ ferrite prepared by self-propagated powders. The SEM pictures of sample sintered at 870^0C/4h had small and homogenous grains (average size less than 1 μm) and pores, while the 900^0C 4h sample had obvious grain growth and few pores.

C. Y. Tsay et al. [83] reported SEM micrographs of Ni-Cu-Zn ferrite (of conventional and microwave sintered) samples posses a very uniform granular structure with grains of size around 1-2 μm.

Zhenxing Yue et al. [84] have synthesized nanocrystalline Ni-Cu-Zn ferrite powders by sol-gel auto combustion method. The SEM photograph of Ni-Cu-Zn ferrite sintered at 900^0 C for Zn is well densified indicating that densification temperature of Ni-Cu-Zn ferrite by

above method is much lower than that of the ferrite prepared by conventional method. From SEM the average grain size determined was about 1-2 μm, exhibiting fine grained microstructure with respect to that of ferrite prepared by conventional route being larger than 10 μm.

Ghodake S. A. [85] investigated the substitution of Ni^{2+} in CuZn ferrite it was found that with the addition of Ni^{2+} the average grain diameter 'D' went on changing and there was no predictable relation between average grain diameter(D) and content of Ni^{2+}.

Most of the grains had sharp grain boundaries indicating that grains were fully developed well packed, crack free with clear grain boundaries. The grain boundaries were distinct and grains were closely packed in some cases which suggested that material had high density and exhibited high magnetization.

2.C.1 Experimental :

The SEM micrographs were obtained from Materials Research Centre, Indian Institute of Science, Bangalore.

The SEM micrographs of the samples are given in Figures 2.C.1 and in the table 2.C.1 data on grain size is given.

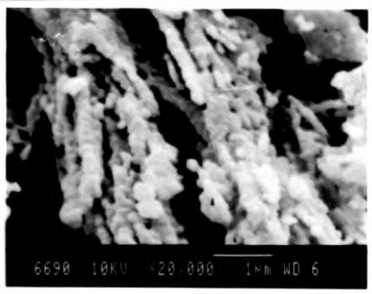

x = 0·1

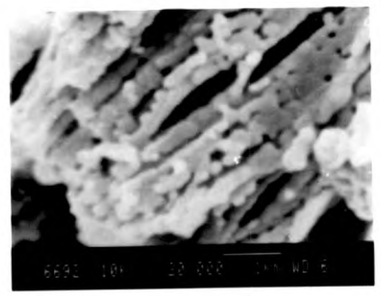

x = 0·2

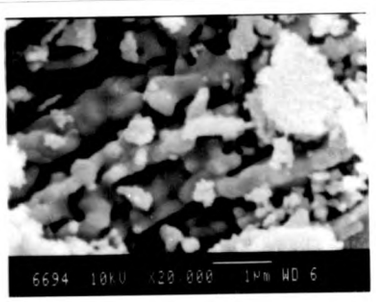

x = 0·3

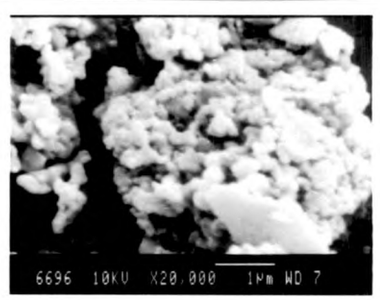

x = 0·4

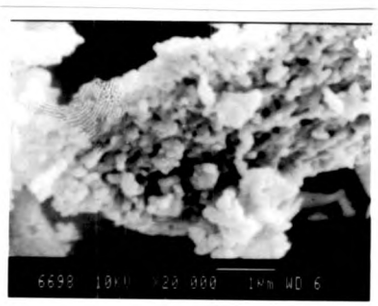

x = 0·5

FIG. 2·C·1 - SEM MIGOGRAPHS FOR $Ni_{0.7-x}Mg_xZn_{0.3}Fe_2O_4$

Table 2.C.1

Data on Grain size according to SEM micrographs

X	μm
0.1	0.143
0.2	0.133
0.3	0.115
0.4	0.095
0.5	0.083

2.C.. Results and Discussion :

It is observed that as the Ni content in the sample decreases the grain size decreases. The grain growth is found to be complete and no exaggerated grain growth is seen. Similar micrographs are also obtained for Zn- Cr, Ni ferrite synthesized from stainless steel making solid waste [87].

PART – D : INFRA-RED STUDIES

INTRODUCTION

Infrared spectroscopy is one of the most powerful analytical techniques which offers the possibility of chemical and structural identification.

Electromagnetic radiations in which wavelengths lie in the range of micron to 1mm are termed as I.R. radiations. It has a wavelength just little longer than that of the visible light. The radiation was discovered by William Hershel in 1800. The electrical and magnetic properties of spinels depend on their chemical composition, cation distribution and the method of preparation. The vibrational, electronic and magnetic dipolar spectra can give information about the position and valancy of the ions in the crystal lattice. The infra-red spectrum is an important non-destructive tool to describe the various ordering problems.

In ferrites, infra-red spectra are used to detect the presence of absorption bands, completion f solid state reaction, study of cation distribution and deformation of the spinel structure.

Waldron [87] was the first to study the infra red spectra of ferrites in a systematic way. He has studied the IR spectra of simple ferrites viz. $ZnFe_2O_4$, $NiFe_2O_4$, $MnFe_2O_4$, $CoFe_2O_4$, $MgFe_2O_4$, Fe_3O_4 in the frequency range 300 – 2000 cm^{-1} and separated out the high frequency electronic spectra from low frequency vibrational spectra. The bands in

the 300 – 700 cm^{-1} region are assigned to the fundamental vibrations of the ions of the crystal lattice.

In case of ferrites the optical spectra gives information about the various vibrational modes in the presence or absence of Fe^{2+} ions in the ferrites whereas the vibrational, electronic and magnetic dipole spectra provide information about the position and the valancy of the ions in the crystal lattice. I. R. spectra are used to detect the presence of absorption or emission bands in the ferrites.

For ferrites the metal ions are situated on two different types of positions, designated octahedral (o) and tetrahedral (t) sites according to the geometrical configuration of the oxygen neighbours. No isolated molecular groupings occur in the structure so the ferrites are assigned to class I or continuously bonded crystals.

Generally spinel ferrites show four active bands ν_1, ν_2, ν_3 and ν_4 in the range of 100 cm^{-1} and 1000 cm^{-1}. The occurrence of these four positions has been rationalised on the basis of group theory. According to Waldron [87] out of the four, two corresponding to high frequencies are broad and asymmetric depending on the preparation conditions and grain size. They give use to distinct shoulder or even splitting of bands. The other two bands corresponding to low frequencies are quite sharp and unaffected by preparation conditions.

Waldron [87] has observed two bands in the region of 200 cm^{-1} to 1000 cm^{-1}. He has attributed the high frequency band ν_1 to tetrahedral complexes and low frequency band ν_2 to octahedral complexes. He has also given the detailed procedure for the calculation of force constants and specific heat of the materials [88].

Hafner [88], Tarte [89] and others [90, 91] investigated the absorption band in many normal and inverse spinel ferrites. Brabers [92] has observed the splitting of bands in cubic and tetragonal Mn ferrites and has concluded that there are local tetragonal distortions, originating from Jahn-Teller effect of the octahedral Mn^{3+} ions. Klerk [93] has observed third fundamental active mode at about 335 cm^{-1} in Mn ferrite. Josyulu [95] et al. have reported four fundamental active mode for Co-Zn ferrite.

2.D.2 Experimental Technique :

The IR spectra of the samples in the present case were obtained from Indian Institute of Science, Bangalore using the Perkin Elmer IR spectrometer (Model 783) in the range 200 cm^{-1} to 800 cm^{-1} in KBr medium.

2.D.3 Results and Discussions :

The IR absorptions of the samples in the series $Ni_{0.7-x}$ Mg_x $Zn_{0.3}$ Fe_2O_4 where x= 0.1, 0.2, 0.3, 0.4 and 0.5 are presented in the figures 2.D.1 and 2.D.2.

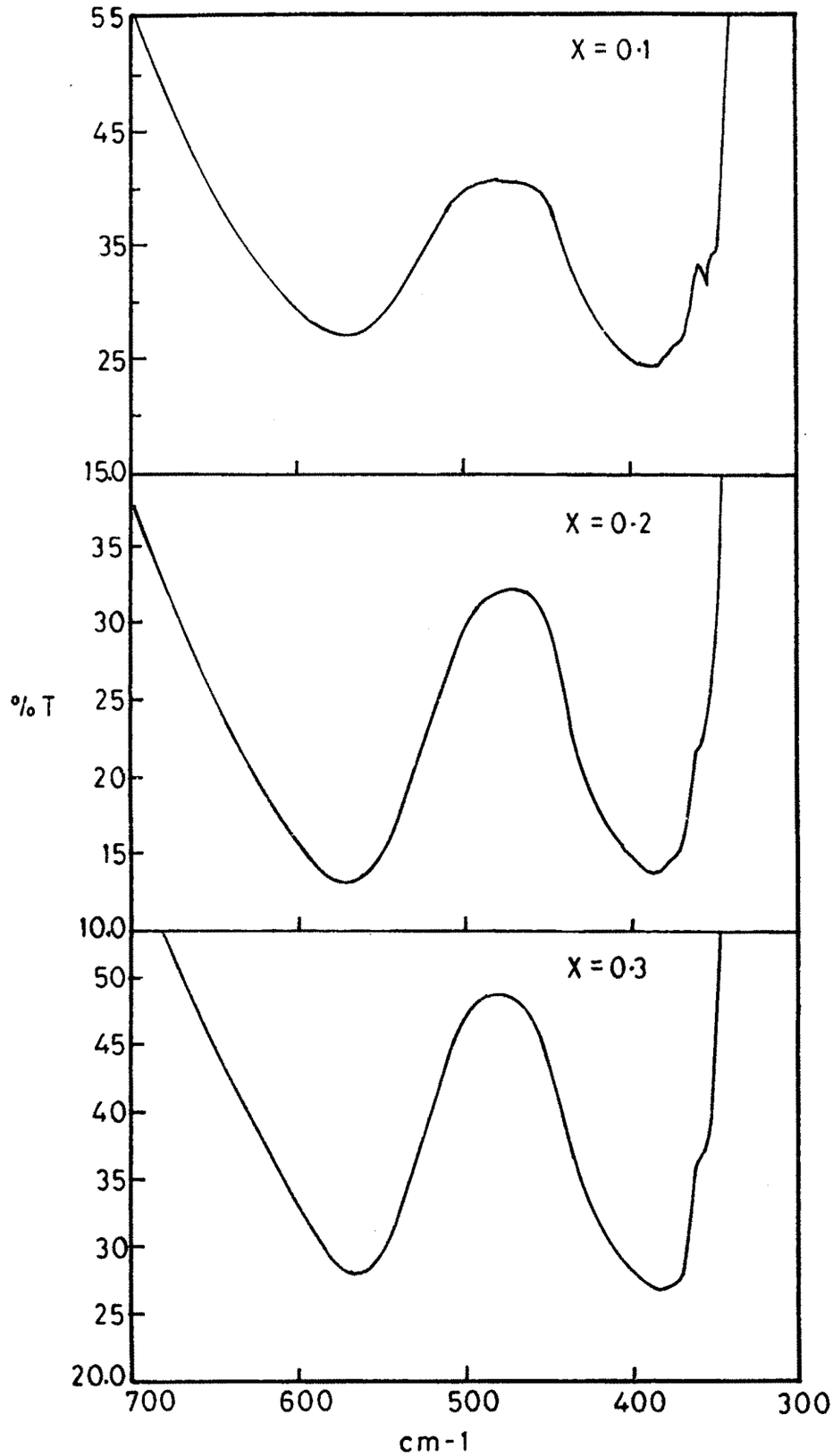

FIG. 2·D·1 - IR SPECTRA OF $Ni_{0.7-x}Mg_xZn_{0.3}Fe_2O_4$

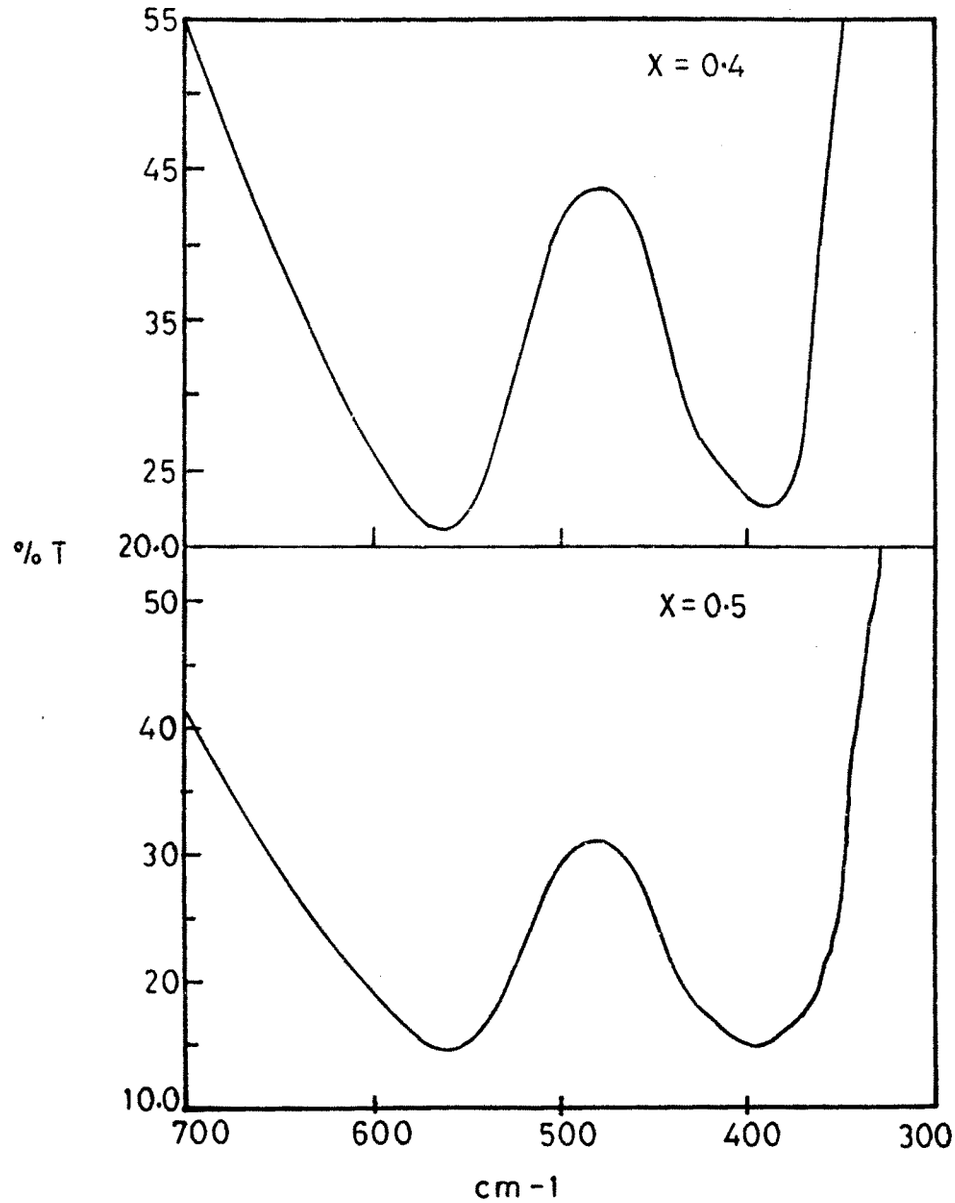

FIG. 2·D·2 - IR SECTRA OF $Ni_{0\cdot8-x}Mg_x Zn_{0\cdot2}Fe_2O_4$

Table 2.D.1 gives the wave numbers of the direct absorption bands in the samples.

Waldron [87] has studied the IR spectra of ferrites and has attributed the band around 600 cm^{-1} to the intrinsic vibrations of the tetrahedral complexes corresponding to the highest restoring force and that around 400 cm^{-1} to an intrinsic vibrations of octahedral complexes which are bond bending vibrations. Therefore it is expected that $\nu_1 > \nu_2$ Hafner [88], White and Anglish [91] have studied IR bands in ferrites and their results support the result of Waldron [87], Tarte and Preudhomme [90] have reported that both ν_1 and ν_2 depend on the nature of octahedral cation significantly but not on the nature of the tetrahedral ions. Potakova et al. [97] have studied the Mossbauer and IR spectra of Ni-Zn ferrites and concluded that Fe^{2+} ions occupy both A and B sites.

Josyulu and Sobhanadri [95] have studied the IR spectra of Co-Zn and Mg-Zn ferrites. They have assigned the ν_3 band near ν_2 to the divalent metal ion –oxygen complexes. The small changes in the band positions have been attributed to the Fe^{3+}- O^{2-} distances in the octahedral and tetrahedral complexes by them.

In the present studies the samples show two prominent bands ν_1 and ν_2 in the range of 600 cm^{-1} to 300 cm^{-1} which are assigned to the vibrations of tetrahedral and octahedral complexes respectively.

It is observed that ν_1 goes on decreasing whereas ν_2 goes on increasing, as the concentration of Mg increases and the concentration of Ni decreases.

The slight change in the positions with composition may be attributed to the change in Fe^{3+} - O^{2-} complexes with the increase of Mg concentration. It suggests that the method of preparation, grain size and porosity can be the influencing factors in locating the band position.

The first three samples show signs of splitting of the ν_2 absorption band. Similar behaviour has been reported by Patil [98] in Zr^{4+} substitution in Cu ferrite. The appearance of splitting in the absorption band around 400 cm^{-1} is assigned to the vibrations of octahedral complexes suggesting the occupancy of B sites by Mg^{2+} ions. The absorption band around 600 cm^{-1} is assigned to the vibrational of tetrahedral complexes does not show any splitting and hence the possibility of Fe^{2+} ions at A sites is ruled out.

Similar results are reported by Pujar [94] in MgZn ferrites. Bhise et al. [99] have studied a similar phenomenon and further the relation of force constants and bond lengths with Zn composition as well as Zirconium substitution in Ni-Zn ferrites.

Table 2.D.1

Absorption Frequencies ν_1 and ν_2 for the samples $Ni_{0.7-x}Mg_xZn_{0.3}Fe_2O_4$

X	ν_1 cm^{-1}	ν_2 cm^{-1}
0.1	570.91	384.90
0.2	571.21	385.47
0.3	564.98	382.28
0.4	564.19	392.07
0.5	561.72	393.25

REFERENCES

1. Anantharaman, T. R. and Suryanarayana, C.

   Rapidly solidified metals a technological overview (Aedermannsd Switzerland : Trans. Tech. Publ. (1987).

2. Libermann, H. H. (ed.)

   Rapidly solidified alloys : process, structures, properties applications (New York : Marcel Dekee Inc.) (1993).

3. Koch, C. C.

   Processing of metals and alloys, Vol. 15 of Materials Science Technology (ed) R.W. Cahn (Weinheim Germany : VCH) pp. 193- (1991).

4. El-Kaddah N. (ed)

   Thermal plasma applications in materials and metallurgical process (Warrendale PA : TMS) (1992).

5. Bickerdike, R. L., Clark, D., Easterbrook, J. N., Hughes, G., Mair, N., Partridge P. G. And Kamson, H. C.

   Int. J. Rapid Solidification, 1305 (1984-85).

6. Turnbull, D.
   Met. Trans A 12695 (1981).

7. Gleiter, H.

   Deformation of polycrypts. Mechanisms and microstructure (eds) Hansen, A Horsewell, T. Leffers and H. Lilholt (Roslilde, Denmar Riso National Laboratory), pp. 15-21 (1981).

8. Bate, G.

Ferromagnetic Materials, Vol. 2, Ed. E.P. Wohlfarth North-Holland Publishing Co., Hague (1980).

9. Siegel, R. W.

MRS Bulletin, 15/60 (1990).

10. Gleiter, H.

Prog. Mater. Sci. 33/223 (1989).

11. Siegel, R. W.

Processing of metals and alloys, Vol. 15 of Material Science and Technology (ed), R.W. Cahn (Weinheim, Germany VCH), pp. 583-614 (1991).

12. Koch, C. C.

Nanostr. Mater. 2109 (1993).

13. Deshpande, C. E. and Date, S. K.

Nanostructured Magnetic Materials.

14. Pileni, M. P.

J. Phys. Chem. 97 (1993) 6961.

15. Chargles, J., O'Connor Nadimir, Kolesnichenko Everett, Carpenter Claudio, Sangregorio Weilie Zhou, Kumbhar Amar, Jessica Sims, Fabrice Agnoli.

Fabrication and properties of magnetic particles with nanometer dimensions synthetic metals 122 (2001) 547-555.

16. Chatterjee, A., Das, D., Pradhan, S. K. and Chakravorty, D.

Synthesis of nanocrystalline Ni-Zn ferrite by the sol-gel method. Journal of Magnetism and Magnetic Materials, 127 (1993) 214-218.

17. Pankor, V. V., Pernet, M., P. Germi P. Mollard.
J. Magn. Magn. Mater. 120 (1993) 69.

18. Kumar, P.S.A., Shrotri, J. J., Deshpande, C. E.
J. Appl. Phys. 81 (1997) 4788.

19. Dias, A., Morara, R. L., Mohallen, N.D.S.
J. Magn. Magn. Mater. 172 (1997) L9- L14.

20. Saha, S. K., Pramanik, P.
Br. Ceram. Trans. 96 (1997) 21-24.

21. Choy, J. H., Han, Y. S.
Mater. Lett. 32 (1997) 209-215.

22. Manoharam, S. S., Patil, K. C.
J. Solid State Chem. 102 (1993) 267-276.

23. Manoharam, S. S., Patil, K. C.
J. Mater. Sci. Lett. 13 (1994) 1711-1714.

24. Gao, Z., Wu, T., Peng, S.
J. Mater. Sci. Lett. 13 (1994) 1715-1716.

25. Park, H. B., Kwon, H. J., Hong, Y. S., Kim, S. J., Kim, K.
J. Mater. Sci. 32 (1997) 57-65.

26. Chakraborty, A., Devi, P. s., Maiti, H. S.
J. Mater. Res 10(4) (1995) 918-925.

27. Shaha, S. K., Pathak, A., Pramanik, P.
J. Mater. Sci. Lett. 14 (1995) 35-37.

28. Lopez-Delgado A., Martin, J. L., Vidales de, Vila, F., Lopez, F. A.
Journal of Alloy and Compds. 281 (198) 312-317.

29. Lopez, F. A., Lozes-Delgado, A., Martin J. L., Vidales de, Vile, E.
Journal of Alloys and Compounds, 265 (1998) 291-296.

30. Patil, K. C. and Mimani, T.
Preparation and properties of nanocrystalline magnetic oxide.

31. Pramanik, P.
Bull. Mater. Sci., Vol. 12, No. 3, May 1999, pp. 335-339.

32. Das, R. N.
Material Letters 47 (2001) 344-350.

33. Lessing, P. A.
Ceram. Bull. 68 (1989) 1002.

34. Swallow, D. and Jordan, A. K.
Proc. Brit. Ceram. Soc. 2 (1964) 1.

35. Dameron, C. T., Resse, R. N., Mehra, R. K., Kortan, A. R., Carroll, P. J., Steigerwald, M. L., Brus, L. F., Winge, D. R.
Nature 338 (1989) 596.

36. Smith, P. R., Holmes, J. P., Richardson, D. J., Russell, D. A., Sodeau J. R.

J. Chem. Soc. Fareday Trans. 94 (1998) 1235.

37. Torimoto, T., Yamashita, M., Kuwabata, S., Sakata, T., Mori, H., Yoneyama, H.

J. Phy. Chem. B. 103 (1999) 8799.

38. Wagner, U.

J. Mag. Mag. Material 19 (1980) 99.

39. Chol, G., Damay, F., Anuradon, J. P. and Strivens, M. P.

Electrical Communications 43 (1968) 263.

40. Stuijts, A. L.

Ferrites Proc. Int. Conf. Japan 108 (1970).

41. Bertaut, M. F.

Comp. Rend. 228 (1949) 492.

42. Warlen, B. E. and Aberbach, B. L.

J. Appl. Phys. 21 (1950) 595.

43. Bragg, W. L.

Nature (London) 95 (1915) 516.

44. Shull, C. G., Wollan, E. O. and Kochlar, W. C.

Phys. Rev. 84 (1952) 912.

45. Hastings, J. M. and Corliss, L. M.

Rev. Mod. Phys. 25 (1953) 114.

46. Prince, E., Treuting, R. G.
Acta. Cryst. 9 (1956) 1025.

47. Cullity, B. P.
"Elements of X-ray diffraction, Wesley Publication Comp. Inc., England 1959.

48. Azaroff, L. V.
Elements Of X-Ray Crystallography, Mcgraw Hill, New York, 1968 And 1974 Ed.

49. Debye, P. and Scherrer, P.
Physica, 17 (1916) 277.

50. Hull, A. W.
Phys. Rev. 9 (1916) 504.

51. Krishnamurthy, K. R.
Ph.D. Thesis, I.I.T., Madras, India (1975).

52. Srivastava, C. M., Srinivasan, G. and Nandikar, N. G.
Phys. Rev. 19 (1979) 499-507.

53. Satyamurthy, N. S., Natera, M. G., Begum, R. G., Youssef, S. I.
Proc. of JCF, Japan (1970).

54. Bhise, B. V., Dongare, M. B., Patil, S. A., Sawant S. R.
J. Mat. Sci. Lett. 10 (1991) 922-924.

55. Srinivasan, T. T., Ravindranathan, P., Cross, L. E., Roy, R., Newnham, R. E., Sankar, S. G. and Patil, K. C.

J. Appl. Phys. 63, 8 (1998) 3789-3791.

56. Deshmukh, U. B.
M. Phil. Thesis. S.U. Centre of Post-graduate Studies, Solapour (1998).

57. Das, R. N.
Materials Letters, 47 (2001) 344-350.

58. Chakravorty, D., Pradhan, S. K., Chatterjee, A.
J. of Magnetism and Magnetic Materials 127 (1993) 214-218.

59. Daruk, O., Yener, Herbert, Giesche.
J. Am. Ceram. Soc. 84(9), 1987-95 (2001).

60. Arcos, D., Velenzuela, R., Vallet-Regi.
J. of solid state Chem. 141 (1998) 10-16.

61. Patil, A. S.
M.Phil. thesis, S.U., Kolhapur (1997).

62. Bradley, F. N.
'Material for Magnetic Functions". Hyden Book Co. Inc. D.B. Taraporewala Sons and Co. Pvt. Ltd. (1980), Chap. 2, pp. 56.

63. Stuijits, A. L.
Proc. Int. Conf. on Ferrites (1970) 1080-113.

64. Browse, A. L., Groenou, Van, Bongers, P. F., Stuijits, a. L.
Mater. Sci. Engg. 3 (1968/69) 317.

65. Went, J., Rathenau, G. N., Gorter, E. W. and Van Osterhaut, G. W.
Phil. Tech. Rev. 13 (1951/52) 194.

66. De Lau, J.G.M.
IEEE Trans. Mgg. 5.

67. VanVleck, L. H.
"Ceramic Microstructure" Edited by Fulratn R. F. and pask J. West View Boulder, Colarado (1976) 4.

68. Lin, I., Nan Mistra, R. K., Thomas, Gareth.
IEEE Trans. On Magnetic MAG 20(1) (1974) 134-139.

69. Globus, A., Duplex, P., Guyot, M.
Roc. Of 1971 "INTERMAG" Conf. Denver Colo (1971) 617-622.

70. Postupolski, T.
Proc. of Fifth Int. Conf. on Ferrites (1989) 639.

71. Roess, E.
"Advances in Ceramics", 15 (1985) 38.

72. Postupolski, T.
Proc. of Third Int. Conf. on Physics of Magnetic Materials Szczyrk-Bila (1986), World Scientific et al. (1987).

73. Postupolski, T.
Prace Institute Telei Raodo technizengo Zerg 107/87 (1988) 1-50.

74. Peloschek, H. P. and Perduijn, D. J.
IEEE Trans. On Magnetics, Vol. MAG 4 Sept. (1968) 453-455.

75. Sundahl, R. C. Jr. Ghate, B. B., Holmes, R. J. and Pass, C. C.
"Advances in Ceramics", 1 (1981) 502.

76. Ravindranathan, P. and Patil, K. C.
J. Mater. Sci. 22 (1987) 3261-3264.

77. Koh, J. G. and Kim, K. U.
New Phys. (Korean Phys. Soc.), Vol. 26(6) (1986) 540-549.

78. Koh, J. G. and Ver, C. I.
New Phys. (Korean Phys. Sci), Vol. 24(4) (1984) 359-371.

79. Murase, T., Igarashi, K., Sawai, J.and Nomura, T.
J. Phys. IV France 7 (1997) Colloque Cl.99-Cl 100 Supplement c
Journal de Physique 111 de Mars (1997).

80. Bhosale, D. N.
Ph.D. Thesis, Shivaji University, Kolhapur, 1997.

81. Nakamura, T.
J. of Mag. And Mcg. Material, 168(1997) 285-291.

82. Hongguo Zhang Zhenwei, Mc Ji Zhou, Zhenxing, You, Longter, L Zhilum, Gui
J. of Mcg. And Mag. Material 213 (2000) 304-308.

83. Tsay, C. Y., Liu, K. S., Lin, T. F., Lin, I. N.
J. of Mag. And Mag. Mater. 209 (2000) 189-192.

84. Zhenxing, You, Zhou, Ji, Longter, Li, Hongguo Zhang, Zhilun, gui.
J. of Mag. And Mag. Mater. 208 (2000) 55-60.

85. Ghodake, S. A.
Ph.D. Thesis, Shivaji University, Kolhapur (2001).

86. Lopez, F. A., Vila, E., Martin de Vidales.
J. of Alloys and Compound 281(1998) 312-317.

87. Waldron, R. D.
Phys. Rev. 99 (1955) 1727.

88. Hafner, S. T.
Z. Fur. Krist 115 (1961) 331.

89. Tarte, p.
Spectrochim Acta 21 (1965) 313.

90. Prudhome J. Spectrochim Acta, 26-A (1970) 985.

91. White, W. B. and Angelish, B. A.
Spectrochim Acta 26-A (1970) 985.

92. Brabers, V.A.M.
Phys. Stat. Solidi (Germany) 33/2 (1969) 563.

93. Klerk, J. and Brabers, V.A.M.
Solid Stat. Commun. (USA) 14/7 (1974) 613.

94. Pujjar .R.B.
Ph.D. Thesis, Shivaji University, Kolhapur.

95. Josyulu, O. and Sobhanadri J.
Phys. Stat. Solidi (a) 65 (1981) 479.

96. Tarte, P., Preudhomme J.
Spectrochim Acta 27(A) (1971) 961.

97. Potakora, V.R., Zverer, N. D.and Romanov, V. P.
Phys. Stat. Solidi (a) 12(1972) 623.

98. Patil, B. L.
Ph.D. Thesis, Shivaji University, Kolhapur (1993).

99. Bhise, B. V., Dongare, M. B., Patil, S. A. and Sawant, S. R.
J. Material Sci. Letter 10(1991) 922.